IEEE Access
Multidisciplinary ⋮ Rapid Review ⋮ Open Access Journal

Received October 18, 2020, accepted November 10, 2020, date of publication November 23, 2020,
date of current version December 8, 2020.

Digital Object Identifier 10.1109/ACCESS.2020.3039921

HVDC Circuit Breakers–A Review

MIKE BARNES[1], (Senior Member, IEEE), DAMIAN SERGIO VILCHIS-RODRIGUEZ[1], (Member, IEEE), XIAOZE PEI[2], (Member, IEEE), ROGER SHUTTLEWORTH[1], (Member, IEEE), OLIVER CWIKOWSKI[3], AND ALEXANDER C. SMITH[1], (Senior Member, IEEE)

[1]Department of Electrical and Electronic Engineering, The University of Manchester, Manchester M13 9PL, U.K.
[2]Department of Electronic and Electrical Engineering, University of Bath, Bath BA2 7AY, U.K.
[3]National Grid, Warwick CV34 6DA, U.K.

Corresponding author: Mike Barnes (mike.barnes@manchester.ac.uk)

This work was supported by the U.K. Research and Innovation Grant EP/L021552/1 FCL/B: An Integrated Fault Current Limiter/Breaker.

ABSTRACT HVDC circuit breakers are of increasing importance, as multi-terminal high voltage DC (HVDC) transmission becomes a commercial reality. Multiple HVDC breaker technologies have been developed, and are starting to appear as proof-of-concept installations on real networks. Information about them is however distributed widely in the literature. This article describes the underlying challenges, the leading candidate solutions, and discusses the requirements and construction of the component sub-assemblies. Its goal is to provide a comprehensive overview of the field.

INDEX TERMS HVDC transmission, circuit breakers, power system protection.

I. INTRODUCTION

High Voltage DC breakers were originally used in Line-Commutated Converter (LCC) HVDC systems [1]–[4]. These breakers had limited capabilities in terms of speed, voltage or current. Solutions to achieve faster, higher-power, DC breakers are of increasing importance though, as multi-terminal VSC HVDC grids develop [5], [6]. A number of such HVDC breaker circuit topologies have been proposed and even trialed as industrial prototypes [7]. However, the development of the technology has been limited by a lack of market: almost all HVDC systems to date have been point-to-point, and the remainder have been small enough not to need HVDC breakers.

With the development of the Zhangbei network [8] however, HVDC grids are reaching new milestones. The development of this, the world's first, large, commercial VSC-HVDC grid, can be expected to spur the development of similar solutions elsewhere. A good review of VSC-HVDC and MVDC breakers was given by [9]–[11], however the technology, applications and understanding of the problems have moved on considerably, and new technologies have been developed since.

The challenge for HVDC breakers is to manage the energy in the electrical system during a fault. Energy stored in the series inductance and shunt capacitance of the DC cables and/or lines must be extracted from the system in order to interrupt the current. In some cases, the AC networks initially feed the DC fault, and this energy too must be dealt with. As a further constraint, any breaker must have both very low losses under normal (unfaulted) conditions, and yet be able to operate very quickly, typically in 2 ms to 10 ms depending on the circumstances. This requires a combination of circuits [2].

This article will provide an overview of faults in DC grids (section II), the fault process (section III), principles of present circuit breakers (section IV), two-circuit solutions (section V), three-circuit solutions (section VI), a summary of circuits (section VII), an overview of sub-assemblies (section VIII) before drawing together key conclusions (section IX).

II. FAULT CLEARING TIMES IN DC GRIDS

At present most VSC HVDC systems are symmetrical monopoles: one converter per station feeding positive and negative voltage DC lines (see section III.B). They are, with few exceptions, point-to-point systems and use underground or subsea DC cables. DC side faults are typically cable faults, therefore faults are rare and will typically be permanent. An extended maintenance period is required during which the entire HVDC link is out of action. Such faults can therefore be dealt with adequately by relatively slow AC breakers [12]. However, for large future multi-terminal systems, this would

The associate editor coordinating the review of this manuscript and approving it for publication was Ali Raza.

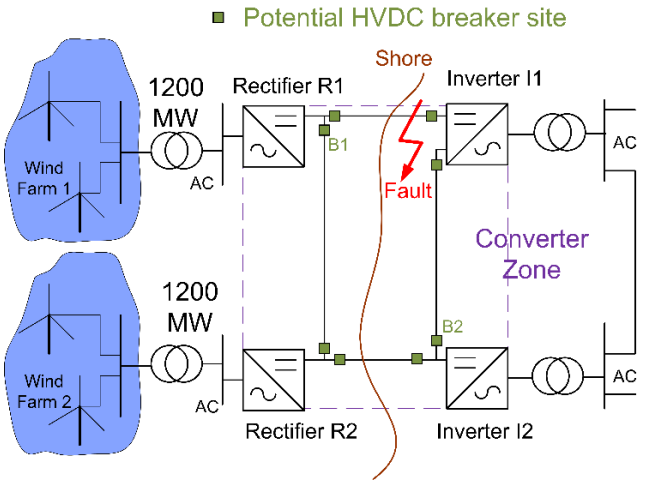

FIGURE 1. Single-line diagram of HVDC scheme with fault and showing converter blocking, fault and potential DC breaker points.

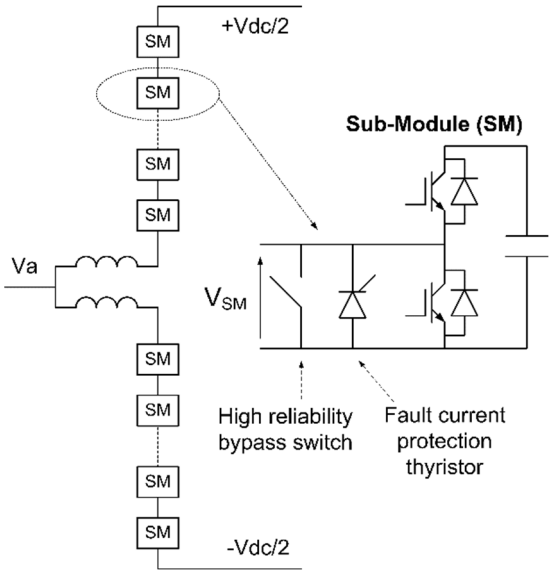

FIGURE 2. One phase of an MMC VSC HVDC, comprising an upper and lower 'arm' – with a Half-Bridge (HB) Sub-Module (SM) shown.

be insufficient. Consider Fig. 1. The AC transmission utility would typically have an agreement defining the maximum power that could be lost due to the outage of a single item of plant. In the UK this is the 'infrequent' loss of generation and is 1800 MW [13]. A fault on a single DC cable could not be allowed to take an entire large DC zone out of action, since this power loss would typically violate the supply infeed constraint (2400 MW in Fig. 1). A DC breaker is thus advantageous to manage the fault. Where overhead lines are used, a DC breaker would be even more advantageous, since faults will be more frequent and may also be temporary.

Some have advocated using a converter capable of blocking during a fault. Conventional VSC-HVDC systems unfortunately do not have fault blocking converters: they use a half-bridge modular multilevel converter (HB-MMC), as shown in Fig. 2. When this tries to block, it in effect becomes a rectifier and so would still feed a DC fault (depending on the type of fault and earthing).

While some topologies such as the full-bridge (FB) MMC can inject a reverse blocking voltage, thus preventing AC from feeding the DC fault [14], they have problems. First, they have greater conduction losses. Then, as in Fig. 1, they still would require the isolation of the entire DC network (the 'Converter Zone' shown by the dashed line), in effect still exceeding the supply infeed loss limit.

It has been suggested that after the FB-MMCs block, fast isolator switches could then remove the isolated section of DC line or cable, and the remaining 'Converter Zone' could be re-energized. Isolators can be smaller and cheaper than breakers, since they only have to switch at zero current. Depending on the type of fault, times of 300 ms to 450 ms have been estimated for this [15], [16]. Where this downtime cannot be tolerated, HVDC breakers will still be needed to isolate the fault before the DC system is disturbed significantly.

In AC protection, a breaker would typically be located at each end of every line, as depicted in Fig. 1. In DC protection this may be undesirable: DC breakers are large, expensive and also require maintenance [17]. They also typically include a series inductor, and the addition of a significant amount of DC inductance can be unhelpful to system stability [15], [18], [19]. A breaker would typically be needed on both positive and negative lines. A better solution has been discussed [15], which separates the DC system into zones – such that the loss of any one zone can be tolerated. In Fig. 1, instead of breakers at each end of every line, only two sets (at B1 and B2) might be needed to split the network into two parts, any one of which might be lost without violating supply limits.

A number of different times are quoted for the required operation time of DC breakers. The breaker must operate quickly enough that it can still break the fault, since breakers have a maximum current rating. As a rough calculation, historically for breakers with a semiconductor element, the peak current carrying capability of the semiconductor breaker (see below) has been assumed to be about 12 kA. For a system with DC line voltages of ±500 kV carrying 2 kA normally, with a 100 mH current limiting inductance, considering a line to ground fault, this leads to a calculation of a required breaking time of:

$$\Delta t = L\frac{\Delta i}{V} = 0.1H\frac{12kA - 2kA}{500kV} = 2ms \tag{1}$$

This may be somewhat conservative. First, circuit breaker designs have risen to 20 kA peak current capability [7]. Second, the system in the above calculation is a large 2 GW system: smaller DC links, ±320 kV, 640 MW (1 kA), would allow longer breaking times. A revised calculation might thus be:

$$\Delta t = L\frac{\Delta i}{V} = 0.1H\frac{20kA - 1kA}{320kV} = 5.9ms \tag{2}$$

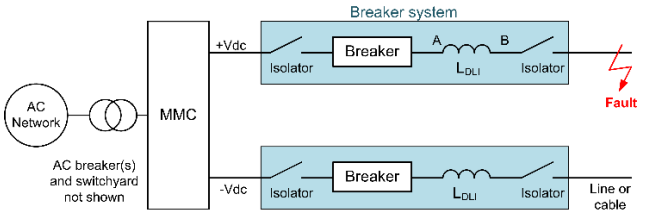

FIGURE 3. Breaker placement with symmetrical monopole MMC. The actual breaker may be placed either side (A or B) of the di/dt limiting inductor (L_{DLI}).

This calculation is only a first estimate. The initial voltage applied to the inductor may be larger as a result of the fault wave (see section III), but the DC voltage will collapse as the fault progresses, resulting in lower fault rate rise times later in the fault period. Also, the MMC arm inductor will be in the fault path, increasing the effective inductance in the calculation.

The breaker must also operate quickly enough that the converter is not damaged. When a conventional HB-MMC blocks, current can continue to flow in the IGBT anti-parallel diode in a manner similar to a conventional two-level converter, and then in the bypass thyristor (if fired). Analysis of a two level converter [20] shows that current stress in these first 5ms is high on the anti-parallel diode. A solution however may be a redesign of the anti-parallel diode set, to increase the permissible breaker operating time, rather than designing a fast breaker to break the fault to avoid problems with the anti-parallel diodes.

A further requirement is that the breaker should operate quickly enough that the remaining DC network is not disturbed to the extent that it has to shut down and be re-energized. The length of time this involves depends on each particular installation. However present research seems to indicate that if the fault can be detected and isolated within circa 10ms, the remaining grid can survive the disturbance [7], [21].

The net result of this is that permissible breaking times may be significantly longer, in the 5-10ms range or more, rather than the 2ms sometimes quoted.

III. THE FAULT PROCESS

A. RATE OF CURRENT RISE

In order to break HVDC currents, a DC breaker system will typically be placed between the converter and DC line (or cable) on both the negative and positive lines, as shown in Fig. 3. Since there is very little inductive impedance on the DC side, the rate of rise of current would be very high during a fault. Hence a DC inductor (L_{DLI}) is typically placed in series with the breaker. In principle the breaker may be placed on either side (A or B) of the inductor, though there are a number of factors to consider (see below). Mechanical isolator switches are also typically added to allow maintenance, and to complete fault isolation, as shown in Fig. 3. This is because a semiconductor switch when 'off' still appears as a high impedance, rather than an isolation gap. The isolator switch would typically be a mechanical switch that can withstand the line voltage rating when open but cannot break current.

Considering the simplest case of a pole to ground fault for a cable, with zero fault impedance, as shown in Fig. 3. The voltage collapses to zero at the point where the fault occurs. This generates a reverse travelling wave from the point of the fault towards the converter [15], [22], [23]. The reverse travelling wave has a peak magnitude of $-V_{DC}$. Any time after the fault, the converter voltage is the sum of the pre-fault DC voltage and the travelling wave. The cable will attenuate the magnitude of the wave as it travels by a factor e^{-kD}, dependent on the attenuation factor (k) and distance (D).

Travelling waves, reaching a discontinuity in their transmission line (cable), will be partly reflected and partly transmitted. If the analysis is undertaken without a DC breaker, the travelling wave will 'hit' the discontinuity formed by the converter equivalent capacitance [24]. In the early days of VSC HVDC this capacitance was large, since a two-level converter was typically used. However once a DC breaker is inserted, the travelling wave will hit the large DC inductance present in all HVDC breakers. Consequently the travelling wave will be reflected, meaning that the cable voltage at B in Fig. 3 becomes negative. In the limit case this means that the current limiting inductor sees twice the DC voltage initially (assuming that the travelling wave is not attenuated). This phenomenon has been widely discussed in the literature [22], [23], [25]–[27]. This in turn means that the initial rate of rise of current will be higher than simple calculations using just V_{dc} would indicate. If the fault is allowed to go on for an extended period, the highest fault current will be reached for the shortest distance D between the fault and the breaker, since this represents the minimum impedance condition. However since a fault will be cleared quickly, the highest fault current seen before the breaker completes its action may be more strongly influenced by the initial rate of rise of current, rather than by the impedance. Thus for fault rating, the worst-case highest current may not be the case of a terminal fault, but a fault some way down the cable [22], [26].

The complexity of the analysis can be treated in a variety of ways. Mathematical analysis on a case-by-case basis is possible [20] but is complicated by the fact that the 'worst-case' may not be a short-circuit terminal fault. Furthermore this worst case may vary as the multi-terminal system is reconfigured and/or evolves. One straightforward scheme to define the required capability of breakers is the use of 'fault current envelopes' [22]. The purpose of these is to define a maximum locus of currents for which to test the breaker. It should be noted that this envelope should exceed the actual fault current the breaker will experience – its function is purely to define a worst case easy-to-test scenario.

A further factor to consider is that the electro-magnetic (EM) fault wave travels along the cable essentially at the speed of an EM wave in the cable medium. The wave will reach the breaker t_f seconds after the fault occurred, but the speed of the wave is such that there is in effect no way to

communicate to the breaker that the fault has occurred before this wave's incidence.

To extinguish the fault, a voltage sufficient to oppose the DC voltage in the fault circuit will be required and to force the current in this circuit to zero in the required time. How to achieve this depends on the topology of the breaker (see below). However, the 'voltage rating' of the breaker needs to take into account not only the injected voltage, but its voltage with respect to ground during the entire fault and post-fault process.

B. INSULATION COORDINATION

The voltage insulation requirements of an HVDC breaker depend on earthing, and the type of fault, [28]. Commonly considered earthing systems include low- and high-impedance grounding, for symmetric monopolar systems and bipolar systems, as shown in Fig. 4. Ground connections might be at the midpoint of one side of a bipolar line, or at the secondary of the transformer. Faults include line-to-line, line-to-line to ground and line-to ground. Typically only one converter is solidly (low-impedance) earthed to avoid ground currents between converters. A good summary of this is given in [6], [15], [28].

The converter also goes through a distinct process. With respect to Fig. 2.

1) The converter is in its pre-fault state: sub-modules have sub-module capacitors inserted by closing a top-switch in the sub-module, or by-passed by closing the bottom switch – either the IGBT or anti-parallel diode may be conducting. Consequently a number of sub-module capacitors are inserted which sum to Vdc across the phase.
2) The converter detects a fault and blocks. All IGBTs are turned off, and conduction is via the bottom diode of the sub-module. Depending on earthing arrangements the AC phase voltage (e.g. V_A) may feed the fault.
3) The sub-module protection fires (e.g. the by-pass thyristor) to reduce the stress on the anti-parallel diode.

In each case, the circuit includes one or more arm inductors.

As an illustration, consider a fault to ground on the positive DC line ($+V_L$) as in Fig. 4. For a solidly earthed bipolar scheme, Fig. 4(a), the inverter DC voltage (V_{INV}) will be applied to the circuit of a whole converter, the DC line, the fault impedance and the ground return path. Effectively the converter DC voltage is shorted. This is half the DC voltage ($2V_L$) of the HVDC scheme. This results in potentially a large fault current contribution from the converter in addition to the fault contribution from the stored energy in the line.

For a symmetrical monopolar scheme, with a Y-to- grounded-Y transformer, Fig. 4(b), the fault circuit is the transformer winding, the arm and arm inductance of the converter connected to the faulted line, the DC line and the ground return path. For a high-impedance earth connected to an artificial mid-point, Fig. 4(c), the (small) top capacitor discharges through the ground path and (excluding other

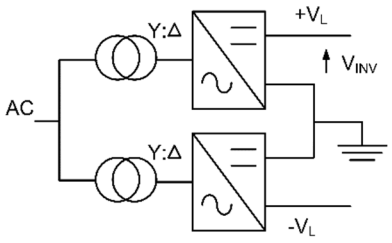

(a) Bipolar (grounded neutral)

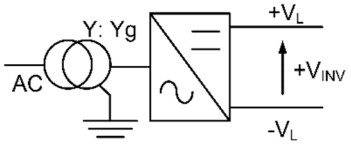

(b) Symmetrical monopolar Y:Y (grounded)

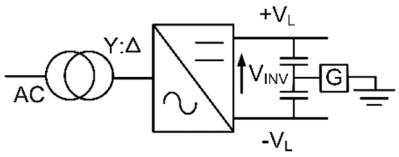

(c) Symmetrical monopolar Y:delta – high impedance ground DC side

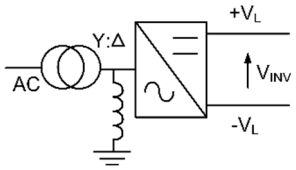

(d) Symmetrical monopolar Y:delta – high impedance ground AC side

FIGURE 4. VSC HVDC configurations and grounding options (not all possible options shown).

protection activity by the converter) the bottom line is pulled towards $-2V_L$ as the top line is pulled to ground. For a symmetrical monopolar converter grounded on the AC side, Fig. 4(d), the discharge path includes a converter arm but the DC negative line is again pulled towards $-2V_L$. Any DC breaker components on these lines must withstand not only the incident fault voltage waveform on the line, but their insulation must also withstand their voltage shift with respect to ground (potentially $-2V_L$ in the case of Fig. 4(c)).

IV. PRIOR ART - PRINCIPLES

Traditionally, HVDC breakers have existed for LCC HVDC. Commercial breakers for LCC HVDC can be divided into four main types [4], [29]:

1) A High Speed Neutral Bus Switch (HSNBS) - This transfers DC current to the ground electrode for faults to ground at the station neutral.
2) A High Speed Ground Switch (HSGS) – This transfers the station neutral to the station grid if the ground electrode becomes isolated.
3) A Metallic Return Transfer Breaker (MRTB) [30] – Under some conditions one pole of a bipolar line can be used as a 'metallic ground return' instead

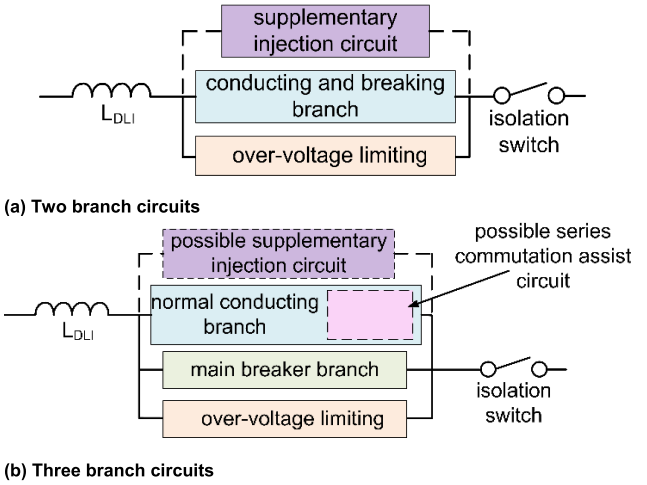

FIGURE 5. HVDC circuit breaker types (supplementary injection circuit optional).

of a positive or negative transmission line. The system is operated as a monopolar link, with the MRTB transferring ground current to the metallic return.

4) Ground (or Earth) Return Transfer Switch (GRTS) – This is the complementary switch to the MRTB. It transfers current from the metallic return to the ground link when the monopolar system is returned to bipolar operation.

However, none of these is required to break full current at full voltage. The MRTB has the highest performance requirements: it is required to interrupt the full DC current, though only at low voltage. The challenge is to achieve low conduction loss, along with fast breaking speed and high breaking voltage (and current).

The concept of dividing breaking into several separate actions of HVDC breakers was discussed as early as 1974 [31]. Solutions have tended to divide into two-branch and three-branch solutions. Two branch solutions have a single branch which conducts and breaks current, and an over-voltage limiting branch (e.g. metal oxide varistors) which limits the voltage across the breaker and absorbs energy. They also will have a rate-of-current-change limiting inductor (L_{DLI}) and a mechanism for supplementary mechanical isolation using a slower isolator switch (or switches). A supplementary circuit may be added to inject current to help the normal conducting branch commutate, as in Fig. 5(a). Three-branch circuits in contrast separate the normal conduction and breaking functions into two parts – a normal low-loss conducting path and a separate path into which current is transferred to break the current, as in Fig. 5(b). The normal conduction path may have a series circuit to aid commutation.

V. TWO-BRANCH CIRCUITS

A. MECHANICAL SWITCH – PASSIVE OSCILLATION

Perhaps the simplest design is based on a higher voltage redesign of the MRTB, using a SF_6 switch as the breaker,

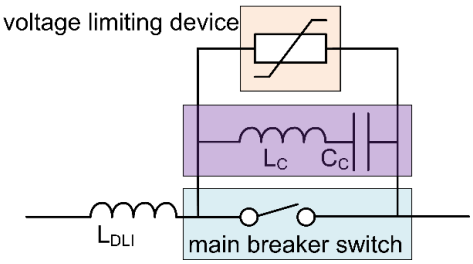

FIGURE 6. Mechanical switch – passive resonance.

with an auxiliary resonant filter, as shown in Fig. 6. When the switch is opened, the switch-arc resulting transfers some current into the filter, and as a result of the arc voltage decreasing with increasing current, a resonant current is superimposed on the switch. When this causes a zero current crossing, the SF_6 switch arc can extinguish, and the switch can be opened. The voltage across the switch then rises until an arrestor is triggered [3], [32]. A field trial extending the operation of this type of unit to 400 kV, and 500 A to 2 kA was undertaken in the 1980's [32] on the Pacific Intertie with commutation times ranging from 2.5 ms to 12 ms. However the combination of only passive resonant elements plus a mechanical switch system may not give sufficiently fast performance for VSC HVDC systems.

Suggestions have been made [33] to slow down current rise by using fault current limiters, for example using superconducting technology. This is an area of substantial research and a good summary of the main issues is given in [34]. Recent work [35] has focused on adapting this circuit – removing L_C and using only L_{DLI} and C_C as the resonant branch.

B. MECHANICAL SWITCH – CURRENT INJECTION

Initial solutions to the HVDC breaker problem tended to use all mechanical switches. To achieve fast commutation, instead of using the arc resistance to create an oscillation, another option using current injection was explored [36]–[38], as for example shown in Fig. 7. The commutating capacitor C_C is precharged by a precharge circuit (made of switches and resistors in that instance). When the commutating switch is closed, an oscillation occurs through an LC circuit, which forces a current zero in the interrupting switch, which can then be opened. The rate of voltage change is limited by a capacitor in parallel to the main breaker switch, and the peak voltage is clamped by the surge arrestor. A further parallel branch may be added, consisting of switched resistors to limit closing overvoltage to the commutation switch. This was used on a 250 kV, 8 kA prototype in the 1980s, in which it was also demonstrated by simulation that a faulted line could be disconnected without interrupting power transmission and the HVDC restored within about 150 ms [38]. The total energy dissipation rating of the surge arrestors was 10 MJ. More recent research, has focused on increasing the speed of the mechanical breaker and thus

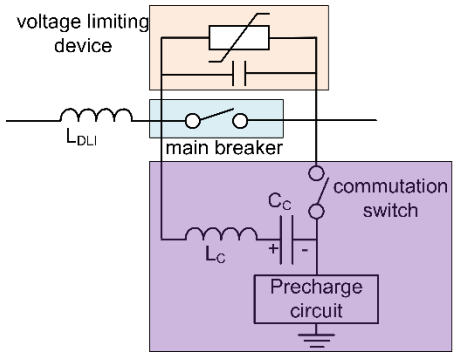

FIGURE 7. Current injection mechanical breaker circuit.

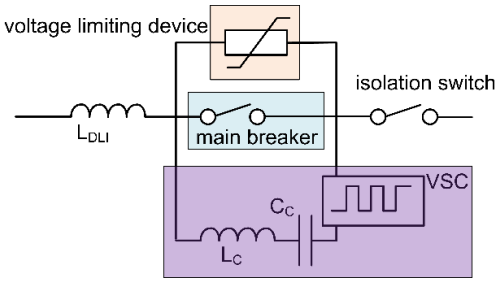

FIGURE 8. Active current injection mechanical breaker circuit.

improving the prospects of the use of such mechanical switch techniques [39]. A variety of current injection breaker, with a different injection circuit was used on the ±160 kV Nan'ao system in China [7] and Mitsubishi have tested a 16 kA breaker [21].

C. MECHANICAL SWITCH – HIGH FREQUENCY RESONANCE

An active resonant injection circuit has also been proposed, [40]–[43]. This principle is shown in Fig. 8. After the main breaker switch is opened and an arc is developed, the excitation circuit is enabled. This is typically a full-bridge voltage source converter (VSC) and applies a high-frequency AC square wave voltage to the LC tank circuit. The oscillating voltage builds the current at each half-wave. Thus a large oscillating current can quickly be built for a relatively small DC voltage on the excitation circuit. Eventually the current in the LC circuit causes the breaker current to reach zero. The breaker arc is extinguished, and current transfers into the inductor and capacitor. The voltage on the capacitor rises until the over-voltage protection device threshold is reached, at which point current transfers to the voltage limiting circuit and the difference in voltage between this and the DC line forces current to zero. At this point the isolation switch opens and isolates the breaker. Typically the voltage on the voltage limiting device is about 1.5 pu, However it has been claimed that much of this can be applied to the inductor and capacitor, with appropriate design. Hence the power electronic components can be rated for a much lower voltage and can be smaller and less expensive.

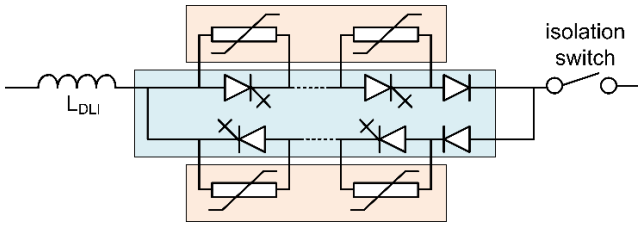

FIGURE 9. Solid-state circuit breaker.

D. SOLID STATE CIRCUIT BREAKER

Solid state circuit breakers use semiconductor switches as both the normally conducting element, and the breaking element. Breakers based on IGBTs, GTOs, IGCTs and other devices have been proposed often initially for medium voltage AC systems, and with a variety of topologies [44]–[46]. To keep conduction losses low, thyristor-derived devices (GTOs and IGCTs) may be preferred. Solutions for medium voltage applications have been proposed. Fig. 9 shows one of the simpler topologies. Since devices can only carry current in one direction, two branches are required in this topology, one for each direction. Not all topologies require two branches.

In Fig. 9 GTOs normally carry current, and turn off in response to a gate signal. Parallel metal oxide varistors limit the voltage applied to each device and dissipate the energy associated with the system during a fault. Diodes may be added to increase the blocking voltage. Again an isolation switch (or one each side to allow maintenance) is needed since voltage devices do not provide full isolation when off. At present, due to the large voltages required, and consequently the large number of series devices needed, the cost of losses prohibits the use of purely semiconductor breakers for HVDC.

E. POWER ELECTRONIC CURRENT INJECTION

In the power electronic current injection circuit breaker [47], [48], Fig. 10, during normal operation, current flows in two mechanical breakers (fast switching vacuum tubes), so called Hybrid Breaking units (HBU). This is consequently a low-loss path. Once a fault is detected, a Pulse Generator (PG) circuit using a thyristor is fired. This pulls the point between the two HBU circuits below ground and draws a large current. This reverses the voltage across the HBU nearest to the fault (assuming some fault impedance and hence voltage drop), and allows the HBU diode(s) to conduct. The HBU switch(es) can then open at zero current. Damping Branches (DB), and snubbers in the PG circuit, then limit over-voltage and absorb energy to remove the fault current.

The PG capacitor is initially charged to the line voltage. When the PG thyristor is fired, this builds current in the PG inductor, until the PG capacitor starts to become reversed biased. This starts to decrease the PG inductor current (in an LC resonance) until eventually the PG thyristor is reverse biased. At this point the PG capacitor is charged by the HBU on the unfaulted side, the voltage on the capacitor rises until

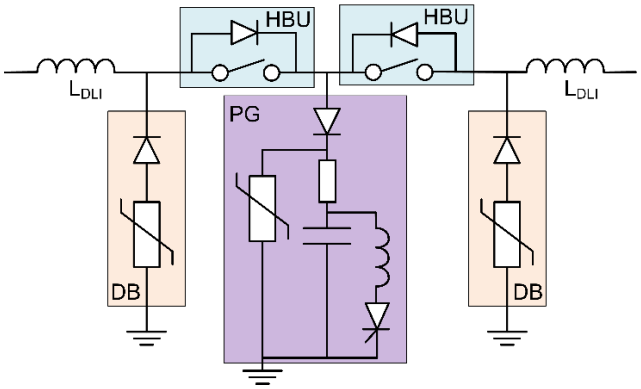

FIGURE 10. Power electronic current injection breaker.

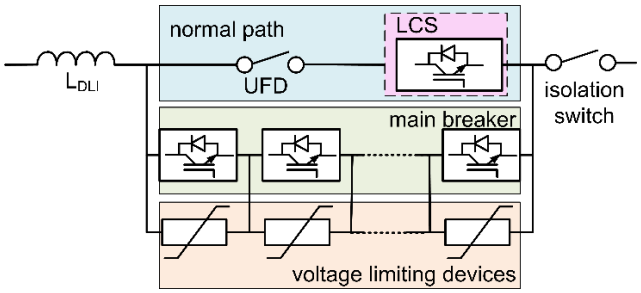

FIGURE 11. ABB proactive hybrid circuit.

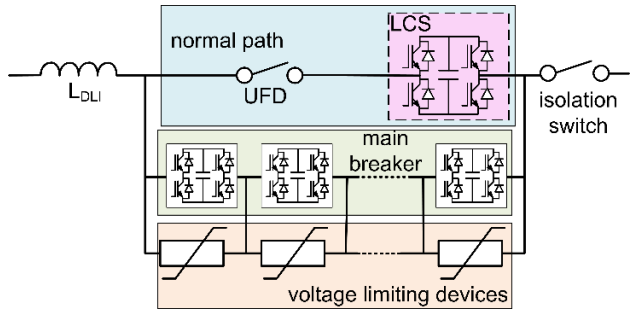

(a) SGCC proactive hybrid breaker circuit

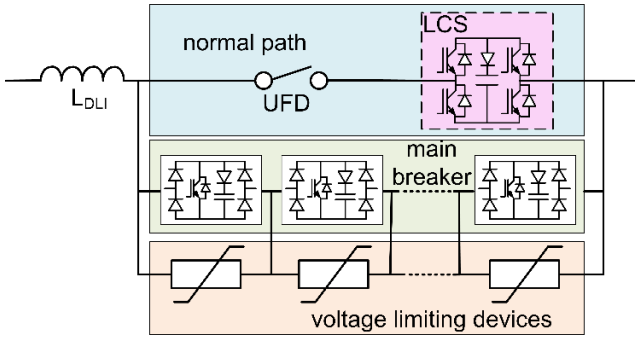

(b) Zhangbei / Global Energy Interconnection Research Institute (GEIRI) proactive hybrid breaker circuit

FIGURE 12. Inherently bidirectional proactive breakers.

the voltage limiting device in the PG is triggered, which reduces current in the HBU on the unfaulted side allowing that switch to open at zero current. The additional isolation switches needed for maintenance are not show in Fig. 10.

VI. THREE-BRANCH CIRCUITS

A. PROACTIVE HYBRID BREAKER

In the hybrid breaker proposed by ABB [49], Fig. 11, current normally flows in a mechanical switch (called the ultra-fast disconnector, UFD) and a power electronic switch (called the load commutation switch, LCS). The normal conduction path is low loss since the UFD is a mechanical device and the LCS is only made up of a few power semiconductor devices and hence has a low on-state voltage drop. In parallel to this is a semiconductor 'main breaker' made of a series connection of multiple power electronic switches, typically IGBTs with anti-parallel diodes. In parallel to both of these is a voltage limiting device, such as a metal oxide varistor.

When a fault is detected, or in proactive operation when a fault is suspected, the main breaker is closed, and the LCS switch is opened. The current transfers to the main breaker, and the UFD can open – this means this mechanical switch opens under effectively no current, and so can operate quickly since it is not required to extinguish an arc. The stray inductance in the circuit limits this transfer and so design for minimal stray inductance is important [50]. Once the voltage withstand across the UFD has been established, the main breaker can open, and current is transferred to the voltage limiting devices which provide a counter voltage to extinguish the fault current.

The 'proactive' aspect of this hybrid breaker arises from the fact that current may be transferred from the UFD and LCS to the main breaker if a fault is suspected. If the fault then fails to materialize, current can be transferred back. The only penalty is the extra losses and heating in the semiconductors of the main breaker during the brief proactive period. The significant advantage is that the mechanical circuit breaker has longer to open and current has been transferred to the main semiconductor breaker earlier, allowing (potentially) a very fast opening time. It can also aid backup protection – should current to the main breaker fail, the proactive operation allows a longer time for a back-up breaker to operate [51].

Much of the delay of this type of circuit is the mechanical switch opening time. Faster mechanical opening times are associated with very significant increased energy requirements to actuate opening, and mechanical constraints may limit maximum opening speed [52]. As for the purely mechanical circuit breaker, an auxiliary circuit to force current to zero in the mechanical switch may be used [52] at the penalty of greater complexity.

Inherently bi-directional variants of the proactive concept have also been proposed, as shown in Fig. 12. The State-Grid Corporation of China (SGCC), Fig. 12(a) [53], [54], designed a 200 kV version for the Zhoushan system (2kA nominal current, 15 kA maximum break current). The load-commutation

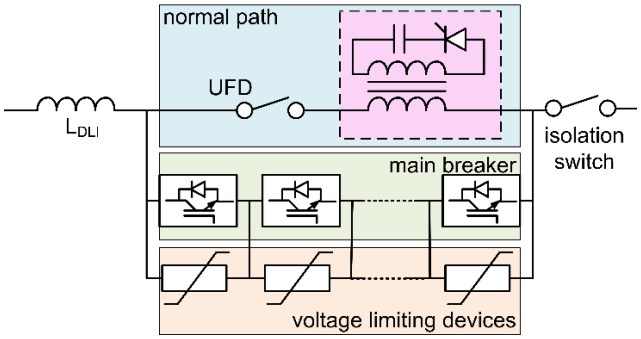

FIGURE 13. Current commutation drive proactive hybrid breaker circuit.

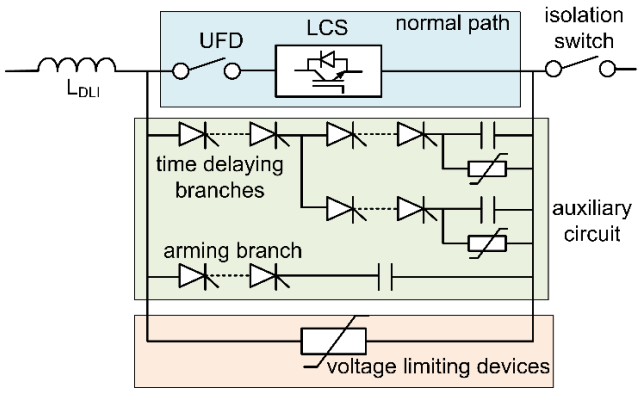

FIGURE 14. Alstom proactive hybrid breaker circuit.

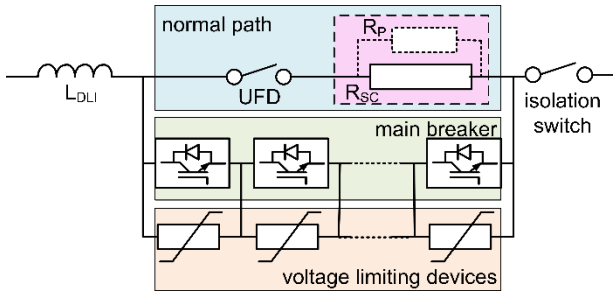

FIGURE 15. Superconductor hybrid breaker.

switch is a full-bridge circuit, allowing bi-directional conduction and circuit blocking. Normally all IGBTs in each LCS circuit cell are turned on, and current flows in two parallel branches of an IGBT and diode. Once the LCS blocks, the DC capacitor is charged through the diodes and acts to transfer current to the main breaker, much like the Proactive Hybrid Breaker above. The main breaker is a series connection of multiple full-bridge cells (connected in 50 kV units in [54]). This allows bi-directional conduction and blocking.

The Zhangbei concept, Fig. 12(b), similarly uses a bidirectional H-bridge circuit as the LCS [8]. The capacitor is in series with a diode, meaning that it acts like a snubber circuit. The capacitor charges through its diode and the IGBT antiparallel diodes when the switches turn off, limiting the rate of rise of voltage across the switches. Similarly, the main breaker path is formed by a series of bidirectional switches: each unit consists of a rectifier bridge, which converts external current in either direction to a unidirectional current applied to an IGBT inside the rectifier. This IGBT can therefore be used to switch bidirectional current. Again a capacitor and diode limit the rate of rise of voltage across the switch when it is turned off.

A further version of the proactive circuit uses a 'current commutation drive circuit', as shown in Fig. 13 [55] instead of an LCS. The thyristor fires when a fault is detected, discharging the pre-charged capacitor, building up a current to counter the main fault current and hence aid commutation of current into the auxiliary circuit.

A variation of the hybrid breaker auxiliary circuit was published by Alstom (now GE) using thyristors and a graded voltage path in the main breaker [56], [57], Fig. 14. The LCS opens, transferring current to time delaying branches. Thyristors fire to insert initially a capacitor branch, which limits the rate of rise of voltage according to the size of capacitor. Once this capacitor has charged up to a set threshold, the second time-delaying branch can be fired – since the capacitor in this second branch is uncharged, current will preferentially transfer to this path in the main breaker, commutating the first set of thyristors. This allows different rates of rise of voltage to be set for different parts of the commutation cycle. It also allows for the voltages of the capacitors in these branches to be less than the peak voltage of the breaker. Two timing branches are shown, but more parallel circuits may be used if desired. Eventually, when the UFD has successfully turned off, and the breaker is to be turned on, the 'arming circuit' is fired and current transfers to this capacitor. The capacitor here is rated for the full blocking voltage, and voltage rises until the extinguishing branch of voltage limiting devices conducts to limit the voltage level. A number of variations on this circuit have been proposed, for example [58]. Also research has been undertaken to investigate other alternatives to semiconductors to achieve the same function as the LCS, for example the physics of constrained current flow in a liquid metal switch [59].

B. SUPERCONDUCTING HYBRID BREAKER

In the simplest form of this breaker, the LCS element of the proactive hybrid breaker is replaced with a superconducting element (R_{SC}) [60], [61], as shown in Fig. 15. During normal operation, the current flows in the mechanical switch and superconducting element, which provides a very low impedance path. The conduction loss in the superconducting element, R_{SC}, is negligible. Once the fault current rises above a threshold (the quench current of the superconducting element), the element stops being superconducting and becomes resistive. The main breaker is turned on (if it has not been proactively turned on before). The voltage drop across the superconducting element acts like the LCS in a proactive hybrid breaker: it diverts the fault current to the lower voltage drop main breaker path. Since R_{SC} is not a pure voltage drop

but a resistance, the UFD has to open while a residual (small) current flows through R_{SC}. The fault current through the mechanical switch is limited by the superconducting element and therefore the current rating of the mechanical switch is reduced compared with that in the proactive hybrid breaker (VI.A). Once the UFD has blocked in the normal path, the main breaker then opens, the voltage limiting devices absorb the residual energy, and finally the isolation switch opens.

In the superconducting hybrid DC circuit breaker, a key advantage is that the superconducting element does not need to withstand the system voltage across its terminals. The superconducting element only needs to withstand a voltage slightly higher than the voltage drop on the main breaker. This greatly reduces the size requirements, and design complexity, of the high voltage termination for the superconducting element. Additional passive elements may be necessary to manage the voltage and current in the circuit, as well as manage the design of the superconducting element – for example a resistance in parallel (R_P) with the element R_{SC}. Normally current flows in the superconducting element. When this stops being superconductive, due to the fault current, some current is diverted into the parallel resistance, reducing the stress on the superconductive element. This parallel resistance however would increase the residual current that the UFD needs to interrupt.

In some circuits [33], [62] the main breaker is removed. In this design the superconductive element and parallel resistance reduce current sufficiently that a mechanical circuit breaker is sufficient to break the DC current, with a voltage limiting element to manage the voltage. Further derivatives exist combining self-oscillation designs with a superconducting element [33]. In this topology, the superconducting element has to the withstand system voltage and the high voltage termination is an essential component.

C. INDUCTIVELY COUPLED HYBRID CIRCUIT

A further option for commutating from the normal to the main breaker path is to use two magnetically coupled windings [63], [64], as shown in Fig. 16. During a fault, the secondary branch (N2) is switched on by closing the main breaker switches. The mechanical switch, UFD, is opened and the arc voltage provides a counter voltage. This voltage and the magnetic coupling between N1 and N2 transfers current to N2. The inductance of N2 is kept lower than N1, so fault current then preferentially builds in the N2. The voltage induced by this rising current helps reduce the primary current. The challenge in this circuit is the competing design constraints on the coupled inductance: low self-inductance to aid commutation requires close coupling, but the need to manage insulation between windings benefits from spacing. Added to this is the need to ensure an appropriate ratio of inductance between the primary and secondary. A supplementary current limiting inductance may still be needed.

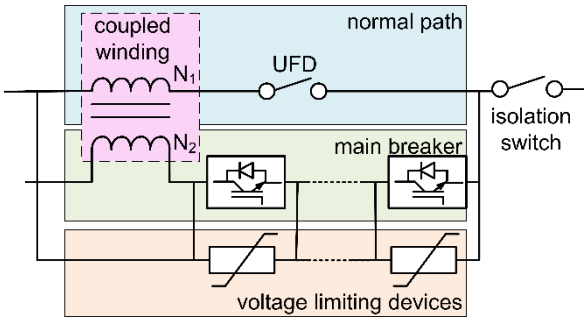

FIGURE 16. Inductively coupled breaker circuit.

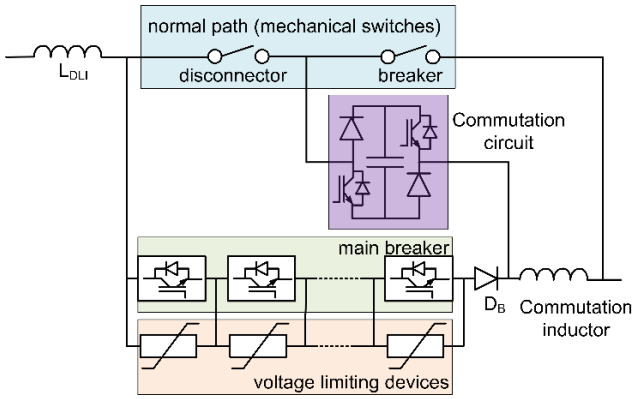

FIGURE 17. Auxiliary capacitor hybrid breaker circuit.

D. AUXILIARY CAPACITOR HYBRID CIRCUIT

A further variant of the hybrid design uses a charged capacitor to divert current from the normal to the main breaker path, as shown in Fig. 17 [65]. This avoids the need for an LCS in the normal path and reduces losses. Current normally flows through the UFD and disconnector. The capacitor in the commutation circuit is precharged. To initiate breaker action, the commutation circuit is fired, and the mechanical circuit breaker is opened. The commutation circuit reduces current in the mechanical breaker switch to zero. The main breaker is closed and the commutation circuit turns off. The mechanical disconnector is opened. Current transfers to the main breaker, which can then be opened, transferring current to the arrestor bank as for other designs. DB is a blocking diode to prevent commutation current flowing back through the main breaker diodes. A 9 kA breaker was demonstrated with a clearing time within 3 ms [65] although only at reduced voltage.

VII. SUMMARY OF CIRCUITS

This article divides solutions for HVDC circuit breakers into several main types, though some have been further developed than others. A brief summary is given in Table 1. Solid-state devices have not been included since they are presently at best suitable for medium voltage applications. Superconducting and inductively coupled devices have not been included since they are still at an early stage of development. Other designs have been proposed in one-off research papers, and may yet provide a step-change in this technology.

TABLE 1. HVDC circuit and examples.

Type	Circuit	Example[1]		
		V /kV	I_{peak} /kA	Site/Source
2 Branch	Mechanical Switch - Passive Oscillation	400	2 [2]	Pacific Intertie [32]
	Mechanical Switch - Current Injection	80 160	10.5 9.2	ABB [39] China Southern Power Grid [7]
	High Frequency Resonance	27	10	SciBreak [43]
	Power Electronic Current Injection	2	10	University of the Bundeswehr [48]
3 Branch	Proactive Hybrid	80 [3] 120 [3] 200 350 535	10 7.5 15 20 26	ABB [51] GE [57] SGRI [54] ABB [66] GEIRI [8]
	Auxiliary Capacitor Hybrid Circuit	ca. 10	9	Toshiba Prototype [65]

1 – Values of Current and Voltage are approximate and for initial ball-park comparison only. Please refer to specific source since values quoted may be measured in different ways.
2 – This is the rated value of the breaker rather than the peak current at commutation.
3 – This is for one cell. Hybrid breakers are multi-cell.

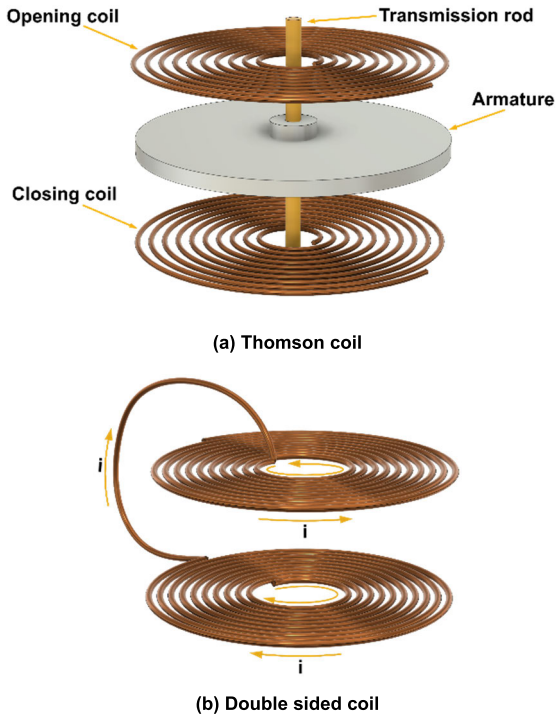

FIGURE 18. Magnetic repulsion based actuators [75].

Table 1 does not give operation times. This is because times often vary with current, which in turn is affected by choice of DC inductance, and a common measurement standard has not been established for times quoted. For example: does the breaking time include detection time? (Some tests do not require detection, but have a triggered breaking instant). As a general guide – the Pacific Intertie has a breaking time of about 12ms given in its paper, the others have times of about 5ms or less quoted in their papers.

The field is evolving rapidly, and the 'best solution' may not yet have been invented. Technology disruptors among sub-components may have a key role to play. These sub-components are discussed in the rest of the paper.

VIII. COMPONENTS

A. THE MECHANICAL SWITCH

All mechanical and hybrid DC breakers use switches with mechanically separable contacts to provide a galvanic barrier in the open state, while providing a low loss conduction path under normal operating conditions. Owing to the time scale differences between electrical and mechanical systems, the opening speed of the mechanical switch has a decisive impact on the breaker isolation time. Therefore the use of an ultra-fast actuator, paired with a robust mechanical switch with excellent dielectric properties, is necessary to expedite and warrant effective operation of hybrid and mechanical DC breakers.

1) ULTRA-FAST ACTUATORS

Mechanical switch opening is one of the most time consuming tasks of an HVDC breaker operation. Isolation times of milliseconds are often suggested as necessary to preserve network integrity in HVDC grids [67] and ultra-fast actuator operation is a topic of utmost research importance [37], [39], [49], [68]–[71]. Given the stringent operational requirements in DC protection applications, magnetic repulsion based actuation mechanisms have been the main research focus in recent publications [69]–[75]. The most common repulsion mechanism used is based on the Thomson coil actuator (TCA) principle.

In its simplest form the TCA consists of spiral coil, with a low number of turns, that interacts with a conductive plate or armature situated in close proximity. To enable bidirectional operation a secondary coil is usually added at the end of the armature travel, as shown in Fig. 18(a). A transmission/insulation rod (to mechanically link the actuated device), a latching mechanism (to keep the actuator in the open and closed positions), a damping system, electric energy storage and control ancillaries are also required for the proper operation of the device. To initiate armature displacement, a time varying current is injected into one of the coils (typically by capacitor discharge), thus producing a time varying magnetic field. The time varying magnetic field induces eddy currents in the conductive armature. Owing to the direction of the induced currents, a repulsive magnetic force between armature and coil is produced. This operating principle allows the construction of fast, compact and robust devices with minimal moving components. Using this design, reaction times of 100μs and opening speeds in excess of 20m/s have been reported for low mass switches [72], [76] and unloaded TC devices [71], [73]. However, for moderately loaded actuators opening speeds in the 5-10 m/s range are more

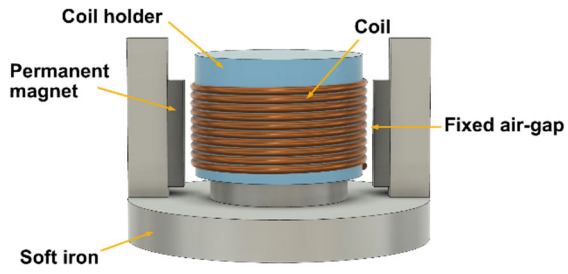

FIGURE 19. Moving coil actuator.

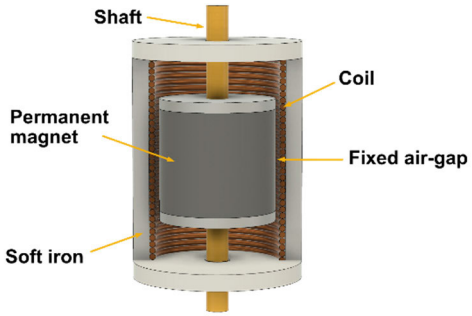

FIGURE 20. Moving magnet actuator.

common [71], [77]. The main drawback of this mechanism is the low efficiency, typically in the 5% range, and the consequent relatively large ancillary components (such as energy storage capacitors) that are required. Additionally, the TC actuator is highly non-linear, thus the force on the moving armature reduces in an approximately inverse square law relationship with displacement.

The TC actuator's poor efficiency is due to the increasing separation between components as the armature moves away from the coil. This separation weakens the magnetic link, thereby diminishing the repulsive force [75]. In order to increase the efficiency alternative, magnetic repulsion drives have been suggested. A magnetic repulsion actuator using a double sided coil arrangement, which does not rely on eddy currents for operation, was proposed in [71], [75]. In this arrangement two series connected flat coils are wound in opposing directions and placed in close proximity. When excitation is applied to the circuit terminals, as shown in Fig. 18(b), the induced magnetic fields result in an opposing force, that drives the coils apart. This alternative design exhibits a marked increase in efficiency over a TC (70% higher), however the overall net efficiency of the design under load remains low, less than 10 % [71]. Thus large capacitors for energy storage are still a requirement. One important drawback of this design is the need for an alternative actuation mechanism to enable bidirectional displacement, complicating the device. Given the low efficiency exhibited by repulsion based actuation technology, actuators with different working principles have been considered for applications where ultra-fast actuation is required [78]–[81].

The moving coil actuator (MCA) consists of a moveable coil immersed in a magnetic field produced by a firmly fixed permanent magnet arrangement, as for example shown in Fig. 19. When excitation is applied to the coil terminals a force proportional to the injected current (Lorentz force) is produced. The generated magnetic forces result in the movement of the coil. The direction of coil movement is dictated by the applied voltage polarity. Thus bidirectional operation of the device can be easily achieved by voltage reversal. Furthermore, since the air-gap between the permanent magnets and the coil remains constant during operation, this device is considerably more efficient than repulsion based actuators [78].

Since the coil is the moving element, a relatively low mass is displaced only. Moving coil type actuators can have sub-millisecond response times. By means of numerical simulations, the dynamic characteristics of the moving coil actuator were found to be adequate for use in HVDC breakers in [78]. However most of the actuator implementations in DC protection schemes have been limited to medium voltage applications [79], [80]. Thus their practicality for use in HVDC breakers still needs to be demonstrated. In addition, complexity and size of the MCA are considerable higher than that of a TC with similar performance.

Another actuator design that has been considered for use in ultra-fast applications is the moving magnet actuator (MMA). The MMA operation principle is similar to that of the MCA. However, in this design the coil is firmly attached to a static surface while the magnet is attached to a moving shaft, as shown in Fig. 20. Due to the exceptional acceleration required in HVDC applications, and the brittle nature of permanent magnet material, the resilience of this kind of device for use in HVDC breakers is questionable. In addition the displaced mass is in general larger than that of an equivalent moving coil actuator, thus a longer reaction time must be expected from a MMA compared to a MCA when subject to similar excitation. The suitability of the MMA for use as an ultra-fast actuator for MVDC protection was investigated in [81], [82], where the lower performance of the MMA compared to a similar MCA was confirmed.

As an alternative to repulsion driven actuators, hydraulic actuators have been implemented in practical HVDC breakers [37]. The pneumatic/hydraulic actuator converts potential energy, typically stored in the form of a high pressure fluid, into linear mechanical motion. High speed valves allow the pressurized fluid access to a cylindrical barrel, where a piston connected to a transmission rod is pushed in the required direction. An opening speed of 10 m/s and less than 3ms response time were reported in [37] for a hydraulic actuator driving a mechanical HVDC breaker. The ability of a hydraulic system to move a 10 kg mass over a distance of 2 cm with a total response time approaching 2.5 ms, at hydraulic pressures up to 340 atm, was reported in [83]. This type of actuator requires a relatively large, robust and complex mechanism in which to store the pressurized fluid and operate the auxiliary valves, making its installation and maintenance in remote locations difficult. Furthermore, similar

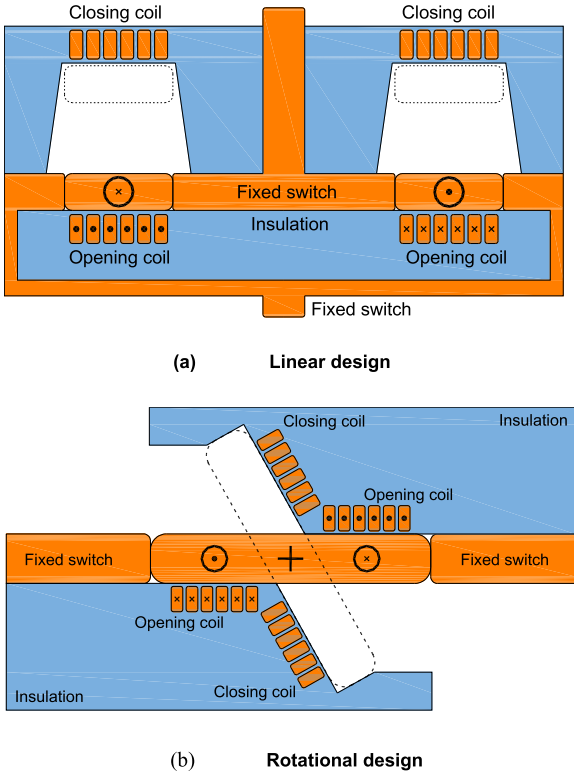

FIGURE 21. Low mass ultra-fast switches [72].

performance figures are achievable using simpler electromagnetic actuators.

Given the limitations in efficiency exhibited by the TCA there is a trend to integrate the latching mechanism [84], [85] with the TC armature as part of the switch design in order to minimize actuator moving mass [72], [76], [77], [86]. Many of these switches can be series connected for voltage scalability [72]. Figure 21 shows linear and rotational switch designs based on this premise.

Although system efficiency remains low with these designs (around 5%), opening velocities of 30 m/s and 50 m/s were reported for the linear and rotational devices, respectively, using a driving energy of approximately 200 J [72]. With this approach, moving mass is minimized. Hence, compared with conventional switches operated by external actuators, the switch reaction time is reduced and the operating speed increases. However, these designs are aimed at medium voltage applications; thus scalability of the switch to HVDC levels needs to be verified. The main challenge, when a number of series connected mechanical switches are used to scale the design to HV levels, is to achieve reliable synchronous operation of all switching elements; otherwise voltage sharing between switch elements can be a concern. Uneven voltage sharing may result in a restrike, and the current interruption process failing.

2) SWITCHING MEDIA

Given the need for fast dielectric recovery, and high insulation strength in HVDC breaker applications, Vacuum Interrupter (VI) and Sulphur Hexafluoride (SF_6) based switches have been favored in practical HVDC breaker designs [36], [49], [51], [37], [87], [88]. Air-blast [32] and oil [89] breakers have also been used as dielectric media in HVDC breakers. However these technologies have fallen into disuse due to the superior dielectric properties of vacuum and SF_6 systems. VIs exhibit high dielectric strength while SF_6 switches possess superior post-arc insulation strength. For these reasons the combined use of series VI and SF_6 interrupters (hybrid switch) has also been suggested as a means to combine the most advantageous properties of each media [90]–[92]. Nevertheless in prototype HVDC breakers a single technology is often used, this is in order to avoid transient recovery voltage (TRV) sharing problems. If the TRV share is disproportionate between interrupters, the switch with the highest voltage may experience an arc restrike. It should be noted that due to its superior insulation strength over vacuum SF_6 has been preferred for voltages above 300 kV; the 320 kV hybrid breaker in [51] uses SF_6 as the insulation media in the mechanical switch.

For medium voltage, VI is the dominant switching technology. Compared with other mechanical switching devices, relatively small gaps are necessary for effective voltage isolation; resulting in a compact design and a small moving mass. The combination of these desirable properties allows for a relatively low energy input requirement for its operation. At medium voltages the VI's breakdown voltage gap characteristic exhibits a linear relationship. However, as the voltage requirement increases, this linearity is lost due to loose electrode micro particles, as indicated in Fig. 22 [93]. In order to extend the usability of VIs to higher voltage levels series connected VIs are often used.

As noted above, for higher voltage levels SF_6 exhibits a superior dielectric strength than vacuum [93], Fig. 23, enabling a more compact switch design. However SF_6 has been identified as a greenhouse gas and due to environmental concerns its use is highly restricted, and alternative strategies to minimize or eliminate it are being developed. For instance, high voltage SF_6 free VIs, up to 145 kV, have been developed [94]; however VI technology use at higher voltages is limited due to cost [95]. Another alternative is to combine SF_6 with other gases, such as N_2, resulting in a significant reduction in the use of SF_6, while preserving its dielectric properties to some extent [96], [97]. From the existing mechanical switching technologies only vacuum and SF_6 (alone or in combination with other gases) switchgear seems able to fulfil the requirements for use in hybrid/mechanical HVDC breakers.

3) GAS-DISCHARGE TUBES

Recently interest has rekindled on the use of gas-discharge tubes as mechanical switches [98]. This, also known as a crossed field switch tube (CFT), is a magnetically controllable gas discharge device in which the ambient pressure is so low than an externally generated magnetic field is required for a discharge to be sustained [99]–[101]. In a CFT conduction

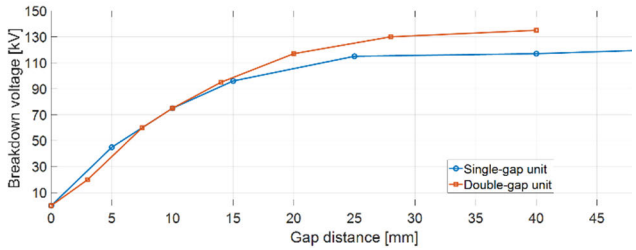

FIGURE 22. Vacuum breakdown voltage gap length characteristic [93].

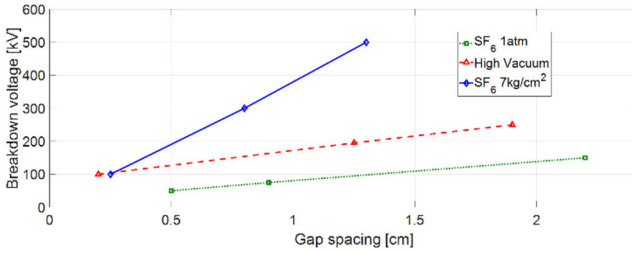

FIGURE 23. SF_6 and vacuum dielectric strength [93].

is possible only if a magnetic field of sufficient strength is applied in a direction perpendicular to the electric field between the electrodes. Thus the removal of the magnetic field will cause the discharge to quench and current flow to cease. Individual and series connected CFTs with a voltage recovery rate around 1-1.5 kV/μs were tested at 100 kV, 1 kA and interruption times of 10 μs were reported [99]. Based on this device HVDC breakers were proposed in [102], [103]. However due to thermal and pressure issues the conduction time of CFTs is limited.

B. THE INDUCTOR

A reactor is typically placed in series with the DC circuit breaker in the DC grid, which is used to limit the rate of rise of the fault current. It is also called the current limiting reactor. A dry-type air-core reactor is normally used to avoid saturation of the magnetic core [104]. The dry-type air-core reactor is environmentally friendly and requires little maintenance. The inductance of the current limiting reactor is determined by the DC system voltage, the main breaker maximum interrupting current, the MMC blocking current, the fault detection and interruption time.

The transient fault current is effectively reduced with a larger current limiting reactor, which allows the DC circuit breaker to have longer time to clear the fault [8]. The reactance is in the range of tens of mH to a few hundred mH depending the HVDC grid voltage [8], [105]. However, the current limiting reactor causes conduction losses and also poses control challenges in the DC grid, which may affect stability of the DC grid [19]. The current limiting reactor also can affect the behaviour of hybrid DC circuit breaker. The impact of the current limiting reactor on the hybrid DC circuit breaker is discussed in detail in [105]. The current limiting reactor can cause overvoltage of the DC circuit breaker after fault interruption. A sudden rate of change of fault current, will generate a large voltage across the DC reactor. This overvoltage added to the DC grid voltage will be applied to the DC circuit breaker when the varistor is absorbing the energy from the system.

Dry-type air-core reactors for HVDC transmission systems normally use cylindrical coils. The parameters considered when designing and testing the dry-type air-core reactor include the inductance, losses, temperature rise of the DC reactor [106], [107]. The inductance of a single layer air-core inductor can be estimated using the following equation [108]:

$$L = \frac{0.001N^2 d}{114d + 254l} \tag{3}$$

where N is the number of turns, d is the diameter of the coil, l is the length of the coil (>0.8 radius). When the length of the coil is longer than the diameter of the coil, the inductance of the reactor can be further simplified using the inductance of a solenoid coil:

$$L = \frac{\mu_0 N^2 A}{l} \tag{4}$$

where μ_0 is the permeability of free space (a vacuum), N is the number of turns, A is the cross-sectional area, l is the length of the solenoid coil.

Dielectric tests and short-circuit withstand tests have to be considered in the design process [106], [107]. The electric field distribution under fault conditions needs to be analyzed to make sure that the maximum electric field is lower than the dielectric strength of the insulation materials. Also the electromagnetic force needs to be investigated to confirm the mechanical integrity under short-circuit fault condition. The electromagnetic force on the conductor follows the Lorentz force law:

$$F = Il \times B \tag{5}$$

It should be noted that the electromagnetic force is proportional to the current squared as the magnetic field flux density also increases with the current. Typically, commercially available dry-type air-core reactor windings are made of large number of aluminum conductors connected in parallel [109]. These conductors are mechanically immobilized and encapsulated in epoxy impregnated fiberglass filaments to enhance the mechanical strength [109]. The dry-type air-core reactors used on HVDC transmission systems are then mounted on insulators rated for the full system voltage, basic insulation level (BIL), and creepage requirements [106], [107].

The DC reactor has also been proposed for use as a means for fast and accurate dc fault detection in a meshed multiterminal HVDC grid [110], [111]. The rate of change of the voltage across the DC reactor is compared with predefined protection voltage thresholds.

In a multiterminal DC grid, there are two options for the locations of the reactors: a centralized configuration

where one reactor is placed next to each MMC converter and a distributed configuration where one reactor is placed on each end of the DC transmission cable [8]. The Zhangbei 500 kV HVDC grid uses a distributed configuration of DC reactors rather than a centralized configuration as the equivalent loop reactance is higher in the first case [8].

C. THE LOAD COMMUTATION SWITCH

The load commutation switch is used to transfer current from the normal conduction path to the main breaker. It must have low losses, a fast switching speed and high reliability. An excellent summary is given in [112].

Typically a fast semiconductor switch is used, for example IGBTs or equivalent devices. An IGBT can conduct in one direction (the direction of the arrow in Fig. 24(a)). The design also only blocks a high voltage in one direction, from collector (high voltage end) to emitter. Since the IGBT can only carry current in one direction, and can only block a low voltage in the reverse direction, a diode is added in parallel allowing current conduction in the reverse direction (i.e. in 'anti-parallel') in Fig. 24(a), and to protect the IGBT from reverse over-voltage.

For a bidirectional switch therefore, a more complex design is required than just a single switch. Fig. 24(b) shows one such example [112]: each IGBT is responsible for carrying current in one direction - S1 for current left to right for example. An extra diode is required in series with each switch to block voltage in the reverse direction: D1 blocks reverse voltage across S1, and prevents D1a conducting, when current is being controlled by the IGBT switch in the other direction. The snubber design to limit overvoltage across the device is complex – conventional designs can cause problems due to oscillation of the snubber capacitance with the stray inductance of the circuit and impact on the speed of the UFD, so more complex designs like Fig. 24(b) are required [112]. Full bridge circuits, as shown in Fig. 12(a), can also be used, though the increased number of series devices may affect conduction losses.

IGBTs have limited peak current carrying and voltage withstand capabilities, with present commercial devices being in the order of several kV and pulsed currents of several kA. For a LCS, a single device would typically not offer sufficient reliability or rating and so the use of several in series and parallel has been proposed. In [49], based on a 4.5 kV StakPak IGBT, a 3-by-3 grid device as shown in Fig. 24(c) was developed. The voltage design required that over-voltage due to stray inductance be considered and a snubber to limit dv/dt be included. To generate enough voltage drop, two devices in series were required (in a test circuit with four 80kV main breaker modules in series, see VII.D). To carry sufficient current, two devices in parallel were required. To allow redundancy an extra series and parallel layer were added forming a 3-by-3 grid. Cooling design was based on a 2-by-2 arrangement carrying current (which results in higher power loss per device) [112].

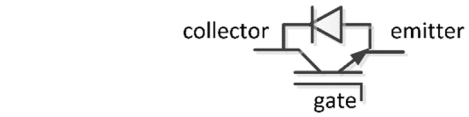

(a) Basic IGBT

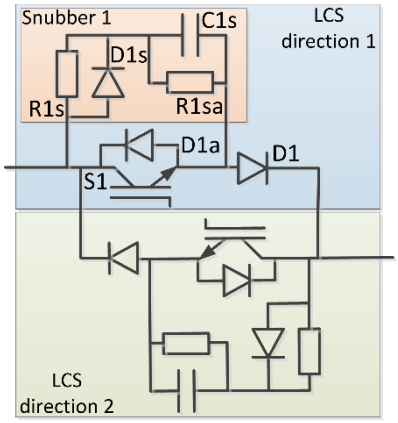

(b) Bi-directional switch circuit (overvoltage arrestor protection not shown)

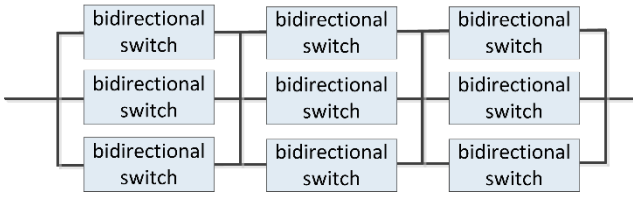

(c) Practical LCS array

FIGURE 24. Load commutation switch elements.

In addition the LCS must be designed for various failures of other parts of the breaker circuit. Fig. 24(c) for example does not show supplementary over-voltage protection.

D. MAIN SEMICONDUCTOR BREAKER

The semiconductor 'main breaker', if used, must carry and break full fault current. It must also withstand the peak voltage applied both by the energy absorbing branch and during any transient which may occur while the breaker is blocked, but has not been isolated from the remaining HVDC system by its isolation switches. Typically it is designed for voltages in excess of 1.5 p.u. [51]. Like the LCS, the main breaker is made of series devices, for example as in Fig. 25, and if necessary parallel devices. The challenge is thus to ensure equal voltage sharing (series) and current (parallel) between switches. Typically the main breaker is modularized. As an example [112] uses 80 kV modules able to interrupt current in either direction, made of 40 IGBT switch modules in each direction. This also allows the main-breaker voltage to be adjusted, if necessary, by inserting all or fewer modules [113]. The use of press-pack devices, ensures failure to a short-circuit if one IGBT fails [51].

Series connection of IGBTs is not straightforward. If turn-on or turn-off rates vary, voltage sharing is not equal

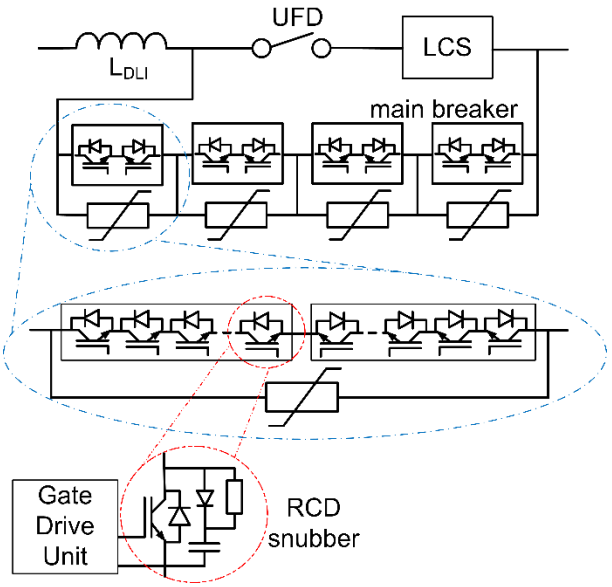

FIGURE 25. Proactive hybrid circuit – main breaker detail.

during transients, potentially damaging devices. In the off-state, if leakage currents and device capacitances and/or resistances are poorly matched, again voltage sharing may be hard to achieve. The literature gives a good review of this quite complex subject [114]–[116], so the detail will not be repeated here. Typically series connected systems use matched devices with some auxiliary passive circuits to assist voltage sharing, where possible. Ideally devices from one production lot would be used to achieve the smallest parameter variation, although close matching of devices in every detail is often impractical [117]. Care must be taken to ensure gate drive pulses are delivered to ensure switching signals are as close to identical as possible, which also means gate lead inductance must be kept as similar as possible. Heating and cooling too ideally would be closely matched to keep device temperature and therefore device resistances, as closely matched as possible. To minimise voltage (Ldi/dt) stress during switching, connection inductance of the switches must be kept low.

Classically, resistors would be placed in parallel with series connected IGBTs to aid static voltage sharing. Since the main breaker is typically used in a hybrid circuit arrangement, it would turn-on at nearly zero voltage and so a turn-on snubber would not be necessary. A combination of resistances, capacitances and diodes (snubbers) would be used to ensure voltages are equalized across series devices during turn-off. However the fast switching of IGBTs may make this more difficult than for slower switching devices [115]. More modern approaches used control of the gate signals to equalize voltages using active feedback [118], though voltage balancing during the 'tail time' of turn-off, when devices are switched off, cannot be balanced by most active control methods, and the use of small snubber circuits may be unavoidable [114]. In any case, main breaker units would need over-voltage protection, and it may be appropriate to combine overvoltage protection (section E) and main breaker modules (see Fig. 13 for example). It should be noted that all these components take up space. All have manufacturing tolerances, which may be significant, especially for capacitors, and may make high precision design of snubbers challenging.

Paralleling devices can be problematic, since devices will have different on-state resistance and voltage drops even if closely matched [114]. Even if devices are closely matched, lead inductance and resistance will affect this transiently and in steady-state. Other factors which can have an important effect include device temperature, which varies resistance, as well as emitter-ground parasitic inductance [114]. Methods to manage this include [114]: derating parallel devices, to allow mismatch – static derating dominates in this consideration; adding series resistance to balance any mismatches (which leads to higher losses); closed loop gate drive control. The complexity of balancing parallel devices, mean that paralleling devices is typically avoided where reasonably possible.

Lastly the breaker will need to be designed for a succession of recurrent operations in case the first is not successful. Reference [113] suggests design for three restart attempts, where the arrester energy handling capability is a key factor. Despite this, it is suggested that cooling of the main breaker devices is not necessary if they are used in a hybrid breaker, as they do not normally carry current [113]. This of course potentially limits the amount of time that current can be proactively transferred to the main breaker.

E. OVERVOLTAGE PROTECTION

Most DC breaker designs rely on metal oxide varistors (MOVs) to limit over-voltages and dissipate the associated energy [39], [49], [33], [119] though there are proposals for devices without them. MOVs are devices with high energy handling capability and voltage clamping properties [120]–[122]. They carry very little (leakage) current until a threshold voltage is reached, above which large current flows (up to a high maximum current density), as shown in Fig. 26. MOVs are highly suited for protection of the solid-state components present in hybrid and solid-state breaker designs, and for energy absorption. Devices can be put in series and share voltage well, however paralleling them is more complex and requires considerable care in finding suitable matching MOVs.

The speed at which a MOV can dissipate energy depends on the energy handling capability of the device. Energy handling capability is defined as the amount of energy that the varistor can absorb before it fails [120]–[122]; this capability is directly related to the device volume [122], [123]. It is clear that for HVDC breaker applications, the faster the operation of the breaker switches, the smaller the energy handling requirement of the MOV, all other things being equal. Furthermore, for the MOV to operate without failure or degradation, the absorbed energy must be quickly dissipated. However in practice the energy and power dissipated

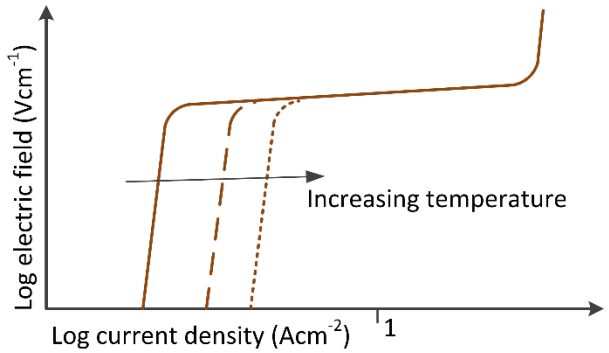

FIGURE 26. Metal oxide varistor characteristic (based on [120]).

must be limited to avoid failure and long term degradation of the MOV electrical properties [122]. The most common MOV failure modes include thermal runaway, puncture and cracking [120].

The response time of a varistor, the time required for the device to respond to a transient overvoltage to provide voltage surge protection, is in the range of 40-60 ns for conventional devices, although faster reacting varistors [124] have also been developed. Their layout, whether in parallel to the device being protected or to ground, also affects MOV system behavior [125], [126].

The use of a varistor results in degradation of the device [127]–[129], noticeable particularly in a moderate increase in the leakage current [127] and a moderate decrease in current for high applied voltages [129]. These changes are however 'acceptable' [129] for DC breaker applications. Environmental conditions too play a role in the aging process of MOVs [130].

The calculation of energy absorbed by the varistor is complex and depends on the AC grid, the DC grid, and converter parameters. Required converter behavior also plays a role [131]. There is also a complex interplay with the design of the effective DC inductance: a larger inductance results in a lower peak fault level, but can result in a longer fault detection time. An increase in inductance may (or may not) result in a higher amount of energy to be absorbed [131]. An excellent summary is given in [132].

Research on this component is limited – and recent work has highlighted that MOVs should be chosen with care [129] – it is clear that this component would benefit from further research.

F. BALANCE OF SYSTEM PLANT

The overall design of the circuit breaker is complex and all issues cannot be adequately covered in a short review article. Key aspects which the designer should bear in mind in addition to main system components are:

- Cooling of power semiconductor switches, particularly for components that carry continuous current needs to be taken into consideration – it is not just conduction losses of the LCS, but also losses in the cooling system and their reliability that must be evaluated [50], [113]. This system must either sit at the voltage of the breaker, or suitable isolation must be achieved.
- The point of adding the circuit breaker into the HVDC circuit is to increase the overall system reliability. However the circuit breaker itself is a complex component with a reliability less than 100%: adding it should not decrease overall system reliability or (at least system availability). These has important implications for the choice of sub-system components and design for redundancy and failure.
- The designs shown have been mostly been unidirectional breakers for one line. Research has been undertaken into making them bidirectional and reducing component count, as well as allowing components to be shared between breakers on adjacent lines. A good summary is given in [50], in essence either two unidirectional breakers are necessary (one for each current direction), or parts of the circuit must be converted into an H-bridge, or put into an external rectifier block (see for example Fig. 12). Recent research papers are also starting to propose multi-port breaker designs which add additional capability (such as current flow control). Again [50] provides a good summary.
- A considerable amount of research has been undertaken into the use of auxiliary fault-current limiting (FCL) devices to further reduce the rate of rise of fault current and to absorb some of the fault energy, therefore reducing the power dissipation in the energy absorption branch. An example is [133] where a resistive FCL is added to the main breaker path. The above point on reliability needs to be considered here.
- Supplying power to components is a key factor – most sit at the voltage of the breaker. Some components (the mechanical switch) require a large amount of energy in a short space of time. Here storage is an option – but this must be sized bearing in mind the potential need for repeated operation in a short space of time.
- Instrumentation, sensors and communication must also be considered – indication of faulty components is required, and the need for potential remote operation should be considered. The complex issue of detection thresholds versus discrimination of faults and robustness against maloperation is a highly complex subject which would benefit from further research.

IX. CONCLUSION

This article has given a review of the main concepts in HVDC breakers, the main contenders for circuits and has described the key sub-assemblies and technologies. An extensive reference list is given. The topic has evolved rapidly in the last few years with multiple solutions now available. The emergence of real-life multi-terminal systems (Nan'ao, Zhoushan and Zhangbei) will undoubtedly spur further research and development.

REFERENCES

[1] V. F. Lescale, A. Kumar, L.-E. Juhlin, H. Bjorklund, and K. Nyberg, "Challenges with multi-terminal UHVDC transmissions," in *Proc. Joint Int. Conf. Power Syst. Technol. IEEE Power India Conf.*, New Dehli, India, Oct. 2008, pp. 1–7.

[2] Cigre Working Group JWG13/14.08, "Circuit-breakers for meshed multiterminal HVDC systems," Cigre, Paris, France, Tech. Rep. 114, 1997.
[3] D. Andersson A. and Henriksson, "Passive and active DC breakers in the three Gorges-Changzhou HVDC project," in *Proc. Int. Conf. Power Syst. (ICPS)*, 2001, pp. 391–395. [Online]. Available: https://library.e.abb.com/public/0f838b2c7ee4629ac1256fda004aeabc/ICPS01Passive.pdf
[4] *IEEE Guide for Establishing Basic Requirements for High-Voltage Direct-Current Transmission Protection and Control Equipment*, IEEE Standard 1899-2017, Jun. 2017, doi: 10.1109/IEEESTD.2017.7959586.
[5] Cigre Working Group B4-72, "DC grid benchmark models for system studies," Cigre, Paris, France, Tech. Rep. 804, 2020.
[6] ABB. (2017). *It's Time to Connect*. [Online]. Available: https://library.e.abb.com/public/285c256c03cd4e168eaae9834ad05c90/PRINTPOW003820R720HR.pdf
[7] D. Jovcic, G. Tang, and H. Pang, "Adopting circuit breakers for high-voltage DC networks: Appropriating the vast advantages of DC transmission grids," *IEEE Power Energy Mag.*, vol. 17, no. 3, pp. 82–93, May 2019, doi: 10.1109/MPE.2019.2897408.
[8] H. Pang and X. Wei, "Research on key technology and equipment for zhangbei 500 kV DC grid," in *Proc. Int. Power Electron. Conf. (IPEC-Niigata-ECCE Asia)*, Niigata, Japan, May 2018, pp. 2343–2351.
[9] C. M. Franck, "HVDC circuit breakers: A review identifying future research needs," *IEEE Trans. Power Del.*, vol. 26, no. 2, pp. 998–1007, Apr. 2011, doi: 10.1109/TPWRD.2010.2095889.
[10] A. Mokhberdoran, H. Leite, A. Carvalho, and N. Silva, "A review on HVDC circuit breakers," in *Proc. 3rd Renew. Power Gener. Conf. (RPG)*, Naples, Italy, 2014, pp. 1–6.
[11] X. Pei, O. Cwikowski, D. S. Vilchis-Rodriguez, M. Barnes, A. C. Smith, and R. Shuttleworth, "A review of technologies for MVDC circuit breakers," in *Proc. IECON-42nd Annu. Conf. IEEE Ind. Electron. Soc.*, Florence, Italy, Oct. 2016, pp. 3799–3805.
[12] Cigre Working Group B4-39, "Integration of large scale wind generation using HVDC and power electronics," Cigre, Paris, France, Tech. Rep. 370, 2009.
[13] (Apr. Mar. 1, 2019). *National Electricity Transmission System Security and Quality of Supply Standard, Version 2.4*. [Online]. Available: https://www.nationalgrideso.com/document/141056/download
[14] C. Petino, F. Schettler, D. Eichhoff, M. Stumpe, M. Heidemann, and E. Spahic, "Application of multilevel full bridge converters in HVDC multiterminal systems," *IET Power Electron.*, vol. 9, no. 2, pp. 297–304, Feb. 2016, doi: 10.1049/iet-pel.2015.0515.
[15] C. D. Barker, R. S. Whitehouse, A. G. Adamczyk, and M. Boden, "Designing fault tolerant HVDC networks with a limited need for HVDC circuit breaker operation," CIGRÉ Paris Session, Paris, France, Tech. Rep. B4-112_2014, 2014.
[16] C. D. Barker and R. S. Whitehouse, "An alternative approach to HVDC grid protection," in *Proc. 10th IET Int. Conf. AC DC Power Transmiss. (ACDC)*, Birmingham, U.K., 2012, pp. 1–6.
[17] C. MacIver, K. R. W. Bell, and D. P. Nedic, "A reliability evaluation of offshore HVDC grid configuration options," *IEEE Trans. Power Del.*, vol. 31, no. 2, pp. 810–819, Apr. 2016, doi: 10.1109/TPWRD.2015.2437717.
[18] W. Wang, M. Barnes, O. Marjanovic, and O. Cwikowski, "Impact of DC breaker systems on multiterminal VSC-HVDC stability," *IEEE Trans. Power Del.*, vol. 31, no. 2, pp. 769–779, Apr. 2016, doi: 10.1109/TPWRD.2015.2409132.
[19] W. Wang, M. Barnes, and O. Marjanovic, "Stability limitation and analytical evaluation of voltage droop controllers for VSC MTDC," *CSEE J. Power Energy Syst.*, vol. 4, no. 2, pp. 238–249, 2018, doi: 10.17775/CSEEJPES.2016.00670.
[20] J. Yang, J. E. Fletcher, and J. O'Reilly, "Multiterminal DC wind farm collection grid internal fault analysis and protection design," *IEEE Trans. Power Del.*, vol. 25, no. 4, pp. 2308–2318, Oct. 2010, doi: 10.1109/TPWRD.2010.2044813.
[21] K. Tahata, H. Ito, R. Yamamoto, K. Kamei, Y. Kono, S. El Oukaili, and D. Yoshida, "HVDC circuit breakers for HVDC grid applications," in *Proc. 11th IET Int. Conf. AC DC Power Transmiss.*, Birmingham, U.K., 2015, pp. 1–9.
[22] O. Cwikowski, R. Shuttleworth, M. Barnes, A. Beddard, and B. Chang, "Fault current testing envelopes for VSC HVDC circuit breakers," *IET Gener., Transmiss. Distrib.*, vol. 10, no. 6, pp. 1393–1400, Apr. 2016, doi: 10.1049/iet-gtd.2015.0863.
[23] W. Leterme, M. Barnes, and D. V. Hertem, "Signal processing for fast fault detection in HVDC grids," *CSEE J. Power Energy Syst.*, vol. 4, no. 4, pp. 469–478, 2018, doi: 10.17775/CSEEJPES.2016.00300.
[24] M. K. Bucher and C. M. Franck, "Analytic approximation of fault current contributions from capacitive components in HVDC cable networks," *IEEE Trans. Power Del.*, vol. 30, no. 1, pp. 74–81, Feb. 2015, doi: 10.1109/TPWRD.2014.2327132.
[25] J. Sneath and A. D. Rajapakse, "DC fault protection of a nine-terminal MMC HVDC grid," in *Proc. 11th IET Int. Conf. AC DC Power Transmiss.*, Birmingham, U.K., 2015, p. 57.
[26] J. Sneath and A. D. Rajapakse, "Fault detection and interruption in an Earthed HVDC grid using ROCOV and hybrid DC breakers," *IEEE Trans. Power Del.*, vol. 31, no. 3, pp. 973–981, Jun. 2016, doi: 10.1109/TPWRD.2014.2364547.
[27] O. Cwikowski, M. Barnes, and R. Shuttleworth, "The impact of traveling waves on HVDC protection," in *Proc. IEEE 11th Int. Conf. Power Electron. Drive Syst.*, Sydney, NSW, Australia, Jun. 2015, pp. 890–897.
[28] W. Leterme, P. Tielens, S. De Boeck, and D. Van Hertem, "Overview of grounding and configuration options for meshed HVDC grids," *IEEE Trans. Power Del.*, vol. 29, no. 6, pp. 2467–2475, Dec. 2014, doi: 10.1109/TPWRD.2014.2331106.
[29] *High Voltage Direct Current Transmission—Proven Technology For Power Exchange*, Siemens AG HVDC Brochure Overview, Erlangen, Germany, 2009.
[30] A. Courts, J. Vithayathil, N. Hingorani, J. Porter, J. Gorman, and C. Kimblin, "A new DC breaker used as metallic return transfer breaker," *IEEE Trans. Power App. Syst.*, vol. PAS-101, no. 10, pp. 4112–4121, Oct. 1982, doi: 10.1109/TPAS.1982.317089.
[31] H. Brumshagen, H. Hartel, and D. Kind, "New developments in design and testing of HVDC circuit breakers," *IEEE Trans. Power App. Syst.*, vol. PAS-93, no. 5, pp. 1353–1358, Sep. 1974, doi: 10.1109/TPAS.1974.293860.
[32] B. Bachmann, G. Mauthe, E. Ruoss, H. P. Lips, J. Porter, and J. Vithayathil, "Development of a 500 kV airblast HVDC circuit breaker," *IEEE Trans. Power App. Syst.*, vol. PAS-104, no. 9, pp. 2460–2466, Sep. 1985, doi: 10.1109/TPAS.1985.318991.
[33] B. Xiang, Z. Liu, Y. Geng, and S. Yanabu, "DC circuit breaker using superconductor for current limiting," *IEEE Trans. Appl. Supercond.*, vol. 25, no. 2, pp. 1–7, Apr. 2015, doi: 10.1109/TASC.2014.2363058.
[34] R. Bini, M. Backman, and A. Hassanpoor, "Interruption technologies for HVDC transmission: State-of-art and outlook," in *Proc. 4th Int. Conf. Electr. Power Equip. Switching Technol. (ICEPE-ST)*, Xi'an, China, Oct. 2017, pp. 318–323.
[35] D. Jovcic, "Series LC DC circuit breaker," *IET High Voltage*, vol. 4, no. 2, pp. 130–137, 2019, doi: 10.1049/hve.2019.0003.
[36] A. Greenwood and T. Lee, "Theory and application of the commutation principle for HVDC circuit breakers," *IEEE Trans. Power App. Syst.*, vol. PAS-91, no. 4, pp. 1570–1574, Jul. 1972, doi: 10.1109/TPAS.1972.293310.
[37] B. L. Damsky, I. Imam, and W. Premerlani, "A new HVDC circuit breaker system design for ±400 kV," in *Proc. 7th IEEE/PES Transmiss. Distrib. Conf. Expo.*, Atlanta, GA, USA, Apr. 1979, pp. 230–236.
[38] S. Tokuyama, K. Arimatsu, Y. Yoshioka, Y. Kato, and K. Hirata, "Development and interrupting tests on 250KV 8KA HVDC circuit breaker," *IEEE Power Eng. Rev.*, vol. PER-5, no. 9, pp. 42–43, Sep. 1985, doi: 10.1109/MPER.1985.5526450.
[39] T. Eriksson, M. Backman, and S. Halén, "A low loss mechanical HVDC breaker for HVDC grid applications," in *Proc. Cigré Session*, 2014, pp. 1–8, paper B4-303.
[40] L. Angquist, S. Norrga, and T. Modeer, "A new DC breaker with reduced need for semiconductors," in *Proc. 18th Eur. Conf. Power Electron. Appl. (EPE ECCE Europe)*, Karlsruhe, Germany, Sep. 2016, pp. 1–9.
[41] L. Angquist, A. Baudoin, T. Modeer, S. Nee, and S. Norrga, "VARC–a cost-effective ultrafast DC circuit breaker concept," in *Proc. IEEE Power Energy Soc. Gen. Meeting (PESGM)*, Portland, OR, USA, Aug. 2018, pp. 1–5.
[42] L. Ängquist, S. Nee, T. Modeer, A. Baudoin, S. Norrga, and N. A. Belda, "Design and test of VSC assisted resonant current (VARC) DC circuit breaker," in *Proc. 15th IET Int. Conf. AC DC Power Transmiss. (ACDC)*, Coventry, U.K., 2019, pp. 3–5.
[43] S. Liu, M. Popov, S. S. Mirhosseini, S. Nee, T. Modeer, L. Angquist, N. Belda, K. Koreman, and M. A. M. M. van der Meijden, "Modeling, experimental validation, and application of VARC HVDC circuit breakers," *IEEE Trans. Power Del.*, vol. 35, no. 3, pp. 1515–1526, Jun. 2020, doi: 10.1109/TPWRD.2019.2947544.

[44] C. Meyer, S. Schroder, and R. W. Dedoncker, "Solid-state circuit breakers and current limiters for medium-voltage systems having distributed power systems," *IEEE Trans. Power Electron.*, vol. 19, no. 5, pp. 1333–1340, Sep. 2004, doi: 10.1109/TPEL.2004.833454.
[45] C. Meyer and R. W. De Doncker, "Solid-state circuit breaker based on active thyristor topologies," *IEEE Trans. Power Electron.*, vol. 21, no. 2, pp. 450–458, Mar. 2006, doi: 10.1109/TPEL.2005.869756.
[46] D. Jovcic and B. Wu, "Fast fault current interruption on high-power DC networks," in *Proc. IEEE PES Gen. Meeting*, Providence, RI, USA, Jul. 2010, pp. 1–6.
[47] Y. Wang and R. Marquardt, "Future HVDC-grids employing modular multilevel converters and hybrid DC-breakers," in *Proc. 15th Eur. Conf. Power Electron. Appl. (EPE)*, Lille, France, Sep. 2013, pp. 1–8.
[48] Y. Wang and R. Marquardt, "Performance of a new fast switching DC-breaker for meshed HVDC-grids," in *Proc. Eur. Conf. Power Electron. Appl.*, Geneva, Switzerland, 2015, pp. 1–9.
[49] J. Häfner and B. Jacobson, "Proactive hybrid HVDC breakers—A key innovation for reliable HVDC grids," in *Proc. Cigré Session*, Bologna, Italy, 2011, pp. 1–8, paper 264.
[50] G. Li, J. Liang, S. Balasubramaniam, T. Joseph, C. E. Ugalde-Loo, and K. F. Jose, "Frontiers of DC circuit breakers in HVDC and MVDC systems," in *Proc. IEEE Conf. Energy Internet Energy Syst. Integr. (EI2)*, Beijing, China, Nov. 2017, pp. 1–6.
[51] M. Callavik, A. Blomberg, J. Häfner, and B. Jacobson, "The hybrid HVDC breaker–an innovation breakthrough enabling reliable HVDC grids," ABB Grid Syst., Tech. Rep., 2012. [Online]. Available: https://library.e.abb.com/public/c9d5ba256e7e9671c1257ab6004b1feb/hybrid-hvdc-breaker—an-innovation-breakthrough-for-reliable-hvdc-gridsnov2012.pdf
[52] C. Meyer, M. Kowal, and R. W. D. Doncker, "Circuit breaker concepts for future high-power DC-applications," in *Proc. Ind. Appl. Conf.*, Hong Kong, vol. 2, 2005, pp. 860–866.
[53] T. Augustin, S. Norrga, and H.-P. Nee, "Modelling of HVDC breakers for HVDC grid simulations," in *Proc. 13th IET Int. Conf. AC DC Power Transmiss. (ACDC)*, Manchester, U.K., 2017, pp. 74-1–74-6.
[54] W. Zhou, X. Wei, S. Zhang, G. Tang, Z. He, J. Zheng, Y. Dan, and C. Gao, "Development and test of a 200kV full-bridge based hybrid HVDC breaker," in *Proc. 17th Eur. Conf. Power Electron. Appl. (EPE ECCE-Europe)*, Geneva, Switzerland, Sep. 2015, pp. 1–7.
[55] W. Wen, Y. Huang, Y. Sun, J. Wu, M. Al-Dweikat, and W. Liu, "Research on current commutation measures for hybrid DC circuit breakers," *IEEE Trans. Power Del.*, vol. 31, no. 4, pp. 1456–1463, Aug. 2016, doi: 10.1109/TPWRD.2016.2535397.
[56] W. Grieshaber, J. P. Dupraz, D. L. Penache, and L. Violleau, "Development and test of a 120 kV direct current circuit breaker," in *Proc. Cigre Paris Session*, Paris, France, 2014, pp. 1–11, paper B4-301.
[57] C. C. Davidson, W. Grieshaber, R. S. Whitehouse, J.-P. Dupraz, and C. D. Barker, "A new ultra-fast HVDC circuit breaker for meshed DC networks," in *Proc. 11th IET Int. Conf. AC DC Power Transmiss.*, Birmingham, U.K., 2015, pp. 47-1–47-7.
[58] A. Beddard and M. Barnes, "Circuit breaker conduction path," Patent P136 908 GB, Aug. 2011.
[59] Y. Wu, Y. Wu, M. Rong, and F. Yang, "Development of a novel HVdc circuit breaker combining liquid metal load commutation switch and two-stage commutation circuit," *IEEE Trans. Ind. Electron.*, vol. 66, no. 8, pp. 6055–6064, Aug. 2019, doi: 10.1109/TIE.2018.2870387.
[60] O. Cwikoski, R. Shuttleworth, and M. Barnes, "Apparatus and Method for Controlling a DC Current," Patent WO 2 014 177 874 A2, May 2014.
[61] X. Pei, O. Cwikowski, A. C. Smith, and M. Barnes, "Design and experimental tests of a superconducting hybrid DC circuit breaker," *IEEE Trans. Appl. Supercond.*, vol. 28, no. 3, pp. 1–5, Apr. 2018, doi: 10.1109/TASC.2018.2793226.
[62] B. Xiang, Y. Tan, K. Yang, Z. Liu, Y. Geng, J. Wang, and S. Yanabu, "Quenched resistance effects on a superconducting current-limiting-type DC breaker," *IEEE Trans. Appl. Supercond.*, vol. 26, no. 7, pp. 1–5, Oct. 2016, doi: 10.1109/TASC.2016.2582660.
[63] J. Magnusson, L. Liljestrand, and R. Saers, "Apparatus arranged to break an electrical current," Patent WO 2 014 032 692, Mar. 6, 2014.
[64] J. Magnusson, R. Saers, and L. Liljestrand, "The commutation booster, a new concept to aid commutation in hybrid DC-breakers," in *Proc. Cigre Session*, Lund, Sweden, 2015, pp. 1–7.
[65] A. Daibo, Y. Niwa, N. Asari, W. Sakaguchi, K. Takimoto, K. Kanaya, and T. Ishiguro, "High-speed current interruption performance of hybrid DCCB for HVDC transmission system," in *Proc. 4th Int. Conf. Electric Power Equip.-Switching Technol. (ICEPE-ST)*, Zhangzhou, China, Oct. 2017, pp. 329–332.
[66] PROMOTioN. *Successful HVDC Circuit Breaker Full-Scale and High-Power Demonstration*. Accessed: Apr. 6, 2020. [Online]. Available: https://www.promotion-offshore.net/news_events/news/detail/successful-hvdc-circuit-breaker-demonstration-unlocks-north-sea-offshore-grid-potential/
[67] Cigre Working Group B4-60, "Designing HVDC grids for optimal reliability and availability performance," Cigre, Paris, France, Tech. Rep. 713, 2017.
[68] A. N. Greenwood, P. Barkan, and W. C. Kracht, "HVDC vacuum circuit breakers," *IEEE Trans. Power App. Syst.*, vol. PAS-91, no. 4, pp. 1575–1588, Jul. 1972, doi: 10.1109/TPAS.1972.293311.
[69] D. Enyuan, W. Yongxing, C. Jiyuan, and Z. Jiyan, "The analysis of high-speed repulsion actuator and performance comparisons with permanent magnetic actuator in vacuum circuit breaker," in *Proc. 23rd Int. Symp. Discharges Electr. Insul. Vac.*, Bucharest, Romania, Sep. 2008, pp. 189–191.
[70] Y. Li, K. Xia, W. Liu, and D. Li, "Design and simulation analysis of electromagnetic repulsion mechanism," in *Proc. Int. Conf. Industrial Technol.*, Vina del Mar, Chile, 2010, pp. 914–918.
[71] A. Bissal, J. Magnusson, and G. Engdahl, "Comparison of two ultra-fast actuator concepts," *IEEE Trans. Magn.*, vol. 48, no. 11, pp. 3315–3318, Nov. 2012, doi: 10.1109/TMAG.2012.2198447.
[72] W. Holaus and K. Frohlich, "Ultra-fast switches—A new element for medium voltage fault current limiting switchgear," in *Proc. IEEE Power Eng. Soc. Winter Meeting. Conf.*, New York, NY, USA, Jan. 2002, pp. 299–304.
[73] V. Puumala and L. Kettunen, "Electromagnetic design of ultrafast electromechanical switches," *IEEE Trans. Power Del.*, vol. 30, no. 3, pp. 1104–1109, Jun. 2015, doi: 10.1109/TPWRD.2014.2362996.
[74] Z. Jian, J. Zhuang, C. Wang, J. Wu, and L. Liu, "Simulation analysis and design of a high speed mechanical contact base on electro-magnetic repulsion mechanism," in *Proc. Int. Conf. Electr. Mach. Syst.*, Beijing, China, Aug. 2011, pp. 1–5.
[75] A. Bissal, J. Magnusson, and G. Engdahl, "Electric to mechanical energy conversion of linear ultra-fast electro-mechanical actuators based on stroke requirements," in *Proc. Int. Conf. Electr. Mach. (ICEM)*, Berlin, Germany, Sep. 2014, pp. 509–515.
[76] M. Steurer, K. Frohlich, W. Holaus, and K. Kaltenegger, "A novel hybrid current-limiting circuit breaker for medium voltage: Principle and test results," *IEEE Trans. Power Del.*, vol. 18, no. 2, pp. 460–467, Apr. 2003, doi: 10.1109/TPWRD.2003.809614.
[77] J.-M. Meyer and A. Rufer, "A DC hybrid circuit breaker with ultra-fast contact opening and integrated gate-commutated thyristors (IGCTs)," *IEEE Trans. Power Del.*, vol. 21, no. 2, pp. 646–651, Apr. 2006, doi: 10.1109/TPWRD.2006.870981.
[78] D. S. Vilchis-Rodriguez, R. Shuttleworth, and M. Barnes, "Finite element assessment of moving coil actuator for HVDC breaker applications," in *Proc. IECON-42nd Annu. Conf. IEEE Ind. Electron. Soc.*, Florence, Italy, Oct. 2016, pp. 4281–4286.
[79] X. Pei, A. C. Smith, R. Shuttleworth, D. S. Vilchis-Rodriguez, and M. Barnes, "Fast operating moving coil actuator for a vacuum interrupter," *IEEE Trans. Energy Convers.*, vol. 32, no. 3, pp. 931–940, Sep. 2017, doi: 10.1109/TEC.2017.2692881.
[80] T. Stroehla, M. Dahlmann, T. Kellerer, T. Wagner, N. Wagner, and T. Sattel, "Ultra-fast moving coil actuator for power switches in medium-voltage grids," *J. Eng.*, vol. 2019, no. 17, pp. 4085–4089, Jun. 2019, doi: 10.1049/joe.2018.8212.
[81] T. Stroehla, M. Dahlmann, T. Sattel, and T. Kellerer, "A model of an ultra—Fast moving magnet actuator for power switches in medium voltage grids," in *Proc. 10th Int. Conf. Electr. Power Drive Syst. (ICEPDS)*, Novocherkassk, Russia, Oct. 2018, pp. 1–6.
[82] B. Yin, X. Pei, X. Zeng, and F. Eastham, "A comparison between moving magnet and moving coil actuators for vacuum interrupters," in *Proc. IECON-45th Annu. Conf. IEEE Ind. Electron. Soc.*, Lisbon, Portugal, Oct. 2019, pp. 5651–5656.
[83] P. Barkan, I. Imam, and W. Premerlani, "A new rapid-response hydraulic actuator—Design, analysis and test results," *J. Mech. Des.*, vol. 102, no. 1, pp. 3–13, Jan. 1980, doi: 10.1115/1.3254718.

[84] P. Skarby and U. Steiger, "An ultra-fast disconnecting switch for a hybrid HVDC breaker—A technical breakthrough," in *Proc. Cigre Conf.*, Calgary, AB, Canada, 2013, pp. 1–9.

[85] D. S. Vilchis-Rodriguez, R. Shuttleworth, A. C. Smith, and M. Barnes, "Design, construction, and test of a lightweight Thomson coil actuator for medium-voltage vacuum switch operation," *IEEE Trans. Energy Convers.*, vol. 34, no. 3, pp. 1542–1552, Sep. 2019, doi: 10.1109/TEC.2019.2905745.

[86] H. Polman, J. A. Ferreira, M. Kaanders, B. H. Evenblij, and P. Van Gelder, "Design of a bi-directional 600 V/6 kA ZVS hybrid DC switch using IGBTs," in *Proc. Conf. Rec. IEEE Ind. Appl. Conf. 36th IAS Annu. Meeting*, Chicago, IL, USA, Sep./Oct. 2001, pp. 1052–1059.

[87] J. M. Anderson and J. J. Carroll, "Applicability of a vacuum interrupter as the basic switch element in HVDC breakers," *IEEE Trans. Power App. Syst.*, vol. PAS-97, no. 5, pp. 1893–1900, Sep. 1978, doi: 10.1109/TPAS.1978.354685.

[88] S. Tokuyama, K. Hirasawa, Y. Yoshioka, and Y. Kato, "Simulations on interruption of circuit breaker in HVDC system with two parallel transmission lines," *IEEE Trans. Power Del.*, vol. 2, no. 3, pp. 772–778, Jul. 1987, doi: 10.1109/TPWRD.1987.4308177.

[89] M. Sakai, Y. Kato, S. Tokuyama, H. Sugawara, and K. Arimatsu, "Development and field application of metallic return protecting breaker for HVDC transmission," *IEEE Trans. Power App. Syst.*, vol. PAS-100, no. 12, pp. 4860–4868, Dec. 1981, doi: 10.1109/TPAS.1981.316449.

[90] S. Yanabu, T. Tamagawa, S. Irokawa, T. Horiuchi, and S. Tomimuro, "Development of HVDC circuit breaker and its interrupting test," *IEEE Trans. Power App. Syst.*, vol. PAS-101, no. 7, pp. 1958–1965, Jul. 1982, doi: 10.1109/TPAS.1982.317441.

[91] T. Senda, T. Tamagawa, K. Higuchi, T. Horiuchi, and S. Yanabu, "Development of HVDC circuit breaker based on hybrid interruption scheme," *IEEE Trans. Power App. Syst.*, vol. PAS-103, no. 3, pp. 545–552, Mar. 1984, doi: 10.1109/TPAS.1984.318743.

[92] C. Xian, L. Minfu, D. Xiongying, and Z. Jiyan, "Development and current status of low-carbon high-voltage large-capacity circuit breaker," in *Proc. Int. Conf. Electr. Control Eng.*, Wuhan, China, Jun. 2010, pp. 3629–3633.

[93] A. Iturregi, E. Torres, I. Zamora, and O. Abarrategui, "High voltage circuit breakers: SF6 vs. Vacuum," in *Proc. Int. Conf. Renew. Energies Power Qual.*, Valencia, Spain, 2009, pp. 1–6.

[94] Siemens News. (Sep. 17, 2019). *Siemens to Provide UK's First SF6 Free 145kV Vacuum Circuit Breakers in Scotland*. [Online]. Available: https://news.siemens.co.uk/news/siemens-to-provide-uks-first-sf6-free-145kv-vacuum-circuit-breakers-in-scotland

[95] R. Renz, "High voltage vacuum interrupters; technical and physical feasibility versus economical efficiency," in *Proc. Int. Symp. Discharges Electr. Insul. Vac.*, Matsue, Japan, Sep. 2006, pp. 257–262.

[96] N. Malik and A. Qureshi, "Breakdown gradients in SF6-n2, SF6-air and SF6-CO2 mixtures," *IEEE Trans. Electr. Insul.*, vol. EI-15, no. 5, pp. 413–418, Oct. 1980, doi: 10.1109/TEI.1980.298335.

[97] Y. Qiu and and E. Kuffel, "Comparison of SF_6/N_2 and SF_6/CO_2 gas mixtures as alternatives to SF_6 gas," *IEEE Trans. Dielectr. Electr. Insul.*, vol. 6, no. 6, pp. 892–895, Dec. 1999, doi: 10.1109/94.822033.

[98] *HVDC Breaker: The Comeback of the Gas-Discharge Tubes*. Accessed: Jan. 29, 2019. [Online]. Available: http://www.think-grid.org/hvdc-breaker-comeback-gas-discharge-tubes

[99] H. Gallagher, G. Hofmann, and M. Lutz, "The crossed field switch tube—A new HVDC circuit interrupter," *IEEE Trans. Power App. Syst.*, vol. PAS-92, no. 2, pp. 702–709, Mar. 1973, doi: 10.1109/TPAS.1973.293775.

[100] M. A. Lutz and G. A. Hofmann, "The Gamitron—A high power crossed-field switch tube for HVDC interruption," *IEEE Trans. Plasma Sci.*, vol. 2, no. 1, pp. 11–24, Mar. 1974, doi: 10.1109/TPS.1974.4316800.

[101] R. J. Harvey and M. A. Lutz, "High power on-off switching with crossed field tubes," *IEEE Trans. Plasma Sci.*, vol. 4, no. 4, pp. 210–217, Dec. 1976, doi: 10.1109/TPS.1976.4316970.

[102] G. A. Hofmann, G. L. La Barbera, N. E. Reed, and L. A. Shillong, "A high speed HVDC circuit breaker with crossed-field interrupters," *IEEE Trans. Power App. Syst.*, vol. 95, no. 4, pp. 1182–1193, Jul. 1976, doi: 10.1109/T-PAS.1976.32212.

[103] G. A. Hofmann, G. L. LaBarbera, N. E. Reed, L. A. Shillong, W. F. Long, and D. J. Melvold, "Field test of HVDC circuit breaker: Load break and fault clearing on the pacific intertie," *IEEE Trans. Power App. Syst.*, vol. 95, no. 3, pp. 829–838, May 1976, doi: 10.1109/T-PAS.1976.32167.

[104] G. Tang, Z. He, H. Pang, X. Huang, and X.-P. Zhang, "Basic topology and key devices of the five-terminal DC grid," *CSEE J. Power Energy Syst.*, vol. 1, no. 2, pp. 22–35, Jun. 2015, doi: 10.17775/CSEEJPES.2015.00016.

[105] J. Martinez-Velasco and J. Magnusson, "Parametric analysis of the hybrid HVDC circuit breaker," *Int. J. Electr. Power Energy Syst.*, vol. 84, pp. 284–295, Jan. 2017, doi: 10.1016/j.ijepes.2016.06.006.

[106] *General Requirements and Test Code for Dry-Type and Oil-Immersed Smoothing Reactors for DC Power Transmission*, IEEE Standard 1277-2000, IEEE Power Energy Society, Feb. 2009.

[107] *General Requirements and Test Code for Dry-Type and Oil-Immersed Smoothing Reactors and for Dry-Type Converter Reactors for DC Power Transmission*, IEEE Standard 1277-2020, IEEE Power Energy Society, May 2020.

[108] H. A. Wheeler, "Simple inductance formulas for radio coils," *Proc. Inst. Radio Eng.*, vol. 16, no. 10, pp. 1398–1400, Oct. 1928, doi: 10.1109/JRPROC.1928.221309.

[109] GE Grid Solutions. *Air-core Reactor*. Accessed: Dec. 4, 2019. [Online]. Available: https://www.gegridsolutions.com/products/brochures/Grid-PEA-L3-ACR-0584-2017_04-EN.pdf

[110] X. Qi, W. Pei, L. Li, and L. Kong, "A fast DC fault detection method for multi-terminal AC/DC hybrid distribution network based on voltage change rate of DC current limiting inductor," *Energies*, vol. 11, no. 7, pp. 1–22, 2018, doi: 10.3390/en11071828.

[111] R. Li, L. Xu, and L. Yao, "DC fault detection and location in meshed multiterminal HVDC systems based on DC reactor voltage change rate," *IEEE Trans. Power Del.*, vol. 32, no. 3, pp. 1516–1526, Jun. 2017, doi: 10.1109/TPWRD.2016.2590501.

[112] A. Hassanpoor, J. Hafner, and B. Jacobson, "Technical assessment of load commutation switch in hybrid HVDC breaker," *IEEE Trans. Power Electron.*, vol. 30, no. 10, pp. 5393–5400, Oct. 2015, doi: 10.1109/TPEL.2014.2372815.

[113] R. Derakhshanfar, T. U. Jonsson, U. Steiger, and M. Herbert, "Hybrid HVDC breaker—Technology and applications in point-to-point connections and DC grids," in *Proc. Cigre Session*, 2014, pp. 1–11. [Online]. Available: https://library.e.abb.com/public/36a26a2c0458fdc9c1257d5d002eb98b/Hybrid%20HVDC%20breaker%20_Technology%20and%20applications%20in%20point-to-point%20connections%20and%20DC%20grids.pdf

[114] N. Y. A. Shammas, R. Withanage, and D. Chamund, "Review of series and parallel connection of IGBTs," *IEE Proc.-Circuits, Devices Syst.*, vol. 153, no. 1, pp. 34–39, Feb. 2006, doi: 10.1049/ip-cds:20050053.

[115] S. Hong, V. Chitta, and D. A. Torrey, "Series connection of IGBT's with active voltage balancing," *IEEE Trans. Ind. Appl.*, vol. 35, no. 4, pp. 917–923, Jul./Aug. 1999, doi: 10.1109/28.777201.

[116] P. R. Palmer and A. N. Githiari, "The series connection of IGBTs with active voltage sharing," *IEEE Trans. Power Electron.*, vol. 12, no. 4, pp. 637–644, Jul. 1997, doi: 10.1109/63.602558.

[117] P. R. Palmer, H. S. Rajamani, and N. Dutton, "Experimental comparison of methods of employing IGBTs connected in series," *IEE Proc.-Electr. Power Appl.*, vol. 151, no. 5, pp. 576–582, Sep. 2004, doi: 10.1049/ip-epa:20040354.

[118] G. Belverde, A. Galluzzo, M. Melito, S. Musumeci, and A. Raciti, "On the series connection of insulated gate power devices," in *Proc. IEEE Int. Caracas Conf. Devices, Circuits Syst.*, Cancun, Mexico, Mar. 2000, pp. P85/1–P85/6.

[119] B. Pauli, G. Mauthe, E. Ruoss, G. Ecklin, J. Porter, and J. Vithayathil, "Development of a high current HVDC circuit breaker with fast fault clearing capability," *IEEE Trans. Power Del.*, vol. 3, no. 4, pp. 2072–2080, Oct. 1988, doi: 10.1109/61.194019.

[120] M. Bartkowiak, M. G. Comber, and G. D. Mahan, "Failure modes and energy absorption capability of ZnO varistors," *IEEE Trans. Power Del.*, vol. 14, no. 1, pp. 152–162, Jan. 1999, doi: 10.1109/61.736708.

[121] M. Bartkowiak, M. G. Comber, and G. D. Mahan, "Influence of nonuniformity of ZnO varistors on their energy absorption capability," *IEEE Trans. Power Del.*, vol. 16, no. 4, pp. 591–598, Oct. 2001, doi: 10.1109/61.956742.

[122] K. G. Ringler, P. Kirkby, C. C. Erven, M. V. Lat, and T. A. Malkiewicz, "The energy absorption capability and time-to-failure of varistors used in station-class metal-oxide surge arresters," *IEEE Trans. Power Del.*, vol. 12, no. 1, pp. 203–212, Jan. 1997, doi: 10.1109/61.568242.

[123] M. M. R. Ahmed, G. A. Putrus, L. Ran, and R. Penlington, "Measuring the energy handling capability of metal oxide varistors," in *Proc. IEE Int. Conf. Exhib. Electr. Distrib.*, Amsterdam, The Netherlands, vol. 1, Jun. 2001, pp. 1–33.

[124] M. A. Weimer and A. W. Weimer, "Novel ultrafast varistor materials for the suppression of fast rise-time transients," in *Proc. IEEE Power Energy Soc. Gen. Meeting-Convers. Del. Electr. Energy 21st Century*, Pittsburgh, PA, USA, Jul. 2008, pp. 1–5.
[125] D. Weiss, N. Drack, M. Duerr, P. Maibach, F. Kirchhoff, and A. Hassanoor, "Design of a surge arrester based load commutation switch for hybrid HVDC breakers," in *Proc. Int. Exhib. Conf. Power Electron., Intell. Motion, Renew. Energy Energy Manage.*, Nuremburg, Germany, 2018, pp. 1–6.
[126] A. Jehle, K. Pally, and J. Biela, "Comparison of energy dissipation concepts for DC circuit breakers," in *Proc. Eur. Conf. Power Electron. Appl.*, Riga, Latvia, Sep. 2018, p. 1.
[127] M. Jaroszewski and J. Pospieszna, "An assessment of ageing of oxide varistors exposed to pulse hazards using dielectric spectroscopy," in *Proc. IEEE Int. Conf. Solid Dielectr.*, Toulouse, France, Jul. 2004, pp. 727–730.
[128] Y. Koga, Y. Yoneda, T. Sato, S. Yokoyama, and S. Matsumoto, "Degradation characteristics on MOV of surge arrester used for 6.6kV power distribution line," in *Proc. 33rd Int. Conf. Lightning Protection (ICLP)*, Estoril, Portugal, Sep. 2016, pp. 1–5.
[129] M. Broker and V. Hinrichsen, "Testing metal–oxide varistors for HVDC breaker application," *IEEE Trans. Power Del.*, vol. 34, no. 1, pp. 346–352, Feb. 2019, doi: 10.1109/TPWRD.2018.2877464.
[130] K. Kannus, K. Lahti, and K. Nousiainen, "Aspects of the performance of metal oxide surge arresters in different environmental conditions," in *Proc. IEE Int. Conf. Exhib. Electr. Distrib.*, Birmingham, U.K., 1997, p. 1–4.
[131] M. Abedrabbo, W. Leterme, and D. Van Hertem, "Systematic approach to HVDC circuit breaker sizing," *IEEE Trans. Power Del.*, vol. 35, no. 1, pp. 288–300, Feb. 2020, doi: 10.1109/TPWRD.2019.2922253.
[132] D. Döring, D. Ergin, K. Würflinger, J. Dorn, F. Schettler, and E. Spahic, "System integration aspects of DC circuit breakers," *IET Power Electron.*, vol. 9, no. 2, pp. 219–227, 2016, doi: 10.1049/iet-pel.2015.0558.
[133] L. Lulu, H. Siquan, H. Kun, L. Chenyang, and H. Qiuling, "A new fast current-limiting HVDC circuit breaker scheme," in *Proc. 2nd IEEE Conf. Energy Internet Energy Syst. Integr. (EI2)*, Beijing, China, Oct. 2018, pp. 1–5.

MIKE BARNES (Senior Member, IEEE) received the B.Eng. degree in engineering and the Ph.D. degree from the University of Warwick, Coventry, U.K., in 1993 and 1998, respectively. He is currently a Professor with The University of Manchester (formerly the University of Manchester Institute of Science and Technology), Manchester, U.K. His principal research interest includes power electronics applied to power systems. He is a Fellow of the Institution of Engineering and Technology, U.K. He is also an Editor of the IEEE TRANSACTIONS ON ENERGY CONVERSION.

DAMIAN SERGIO VILCHIS-RODRIGUEZ (Member, IEEE) received the Ph.D. degree in electrical engineering from the University of Glasgow, Glasgow, U.K., in 2010. He was a Computer Programmer and a Power Quality Consultant in Mexico, from 1993 to 2004. He is currently a Senior Research Associate with the Power and Energy Division, The University of Manchester, Manchester, U.K. His current research interests include electrical machines modeling, condition monitoring of rotating ac machinery, power systems simulation, high-voltage dc protection, and reliability analysis of HVDC systems.

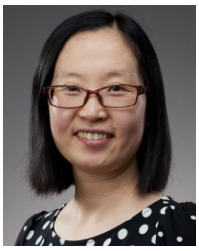

XIAOZE PEI (Member, IEEE) received the B.Eng. and M.Eng. degrees from Beijing Jiaotong University, Beijing, China, in 2006 and 2008, respectively, and the Ph.D. degree from The University of Manchester, Manchester, U.K., in 2012. She became a Research Associate with The University of Manchester. In 2017, she joined the University of Bath, as a Lecturer. She has extensive research experience in designing and building of superconducting fault current limiters and fast operating vacuum circuit breakers. Her research interests include electrical power applications of superconductivity and hybrid dc circuit breaker.

ROGER SHUTTLEWORTH (Member, IEEE) was born in U.K. He received the B.Sc. and Ph.D. degrees in electrical and electronic engineering from The University of Manchester. He worked for a year at GEC Traction before joining the University as a Lecturer with the Power System's Research Group and later the Power Conversion Research Group. He was the Director of the Power Electronics, Machines and Drives M.Sc. course at The University of Manchester, until 2016. He retired in 2017. He has more than 100 articles and patents. His main research interests include power electronics, energy control and conversion, HVDC, circuit breaking, and energy harvesting.

OLIVER CWIKOWSKI was born in OH, USA, in 1989. He received the M.Eng. degree (Hons.) in electrical and electronic engineering and the Ph.D. degree in electrical and electronic engineering from The University of Manchester, in 2012 and 2016, respectively. He is currently a Senior Innovation Engineer with National Grid Electricity Transmission, where he leads underground transmission innovation. He is a member of the IET.

ALEXANDER C. (SANDY) SMITH (Senior Member, IEEE) received the B.Sc. (Eng.) and Ph.D. degrees from Aberdeen University, U.K., in 1977 and 1980, respectively. His previous academic appointments were at the Imperial College London and Cambridge University. He joined Invensys Brook Crompton, in 1997, as the Head of Research for motor technology. He is currently a Professor of electrical machines with The University of Manchester and the Director of the Roll-Royce University Technology Centre on Electrical Systems for Extreme Environments. His research interests include design and modeling of motors, generators, superconducting machines, and electrical drive systems. He is a Fellow of the Institute of Engineering and Technology. He was the Editor-in-Chief of the *IET Electrical Systems in Transportation* journal.